Resveratrol inhibits growth of experimental abdominal aortic aneurysm associated with upregulation of angiotensin converting enzyme 2

Corey S Moran[1], Erik Biros[1], Smriti M Krishna[1], Yutang Wang[2], Chris Tikellis[3], Joseph V Moxon[1], Mark E Cooper[3], Paul E Norman[4], Louise M Burrell[5], Merlin C Thomas[3], Jonathan Golledge[1,6]

[1]The Vascular Biology Unit, Queensland Research Centre for Peripheral Vascular Disease, College of Medicine and Dentistry, James Cook University, Townsville, Queensland, Australia; [2]School of Applied and Biomedical Sciences, Faculty of Science and Technology, Federation University Australia, Mount Helen, Victoria, Australia; [3]Department of Diabetes, Central Clinical School, Monash University, Melbourne, Victoria, Australia; [4]School of Surgery, University of Western Australia, Fremantle Hospital, Fremantle, Western Australia, Australia; [5]Department of Medicine, The University of Melbourne, Austin Hospital, Melbourne, Victoria, Australia; [6]The Department of Vascular and Endovascular Surgery, The Townsville Hospital, Townsville, Queensland , Australia.

Running Title – Moran; Resveratrol and ACE2 in AAA

Address for correspondence: Professor Jonathan Golledge, The Vascular Biology Unit, Queensland Research Centre for Peripheral Vascular Disease, College of Medicine and Dentistry, James Cook University Townsville, QLD, Australia 4811. Fax +61 7 4796 1401 Telephone +61 7 4796 1417 Email: jonathan.golledge@jcu.edu.au

Key Words: aneurysm, apolipoprotein E-null mouse, resveratrol, angiotensin II, angiotensin-converting enzyme 2, vascular smooth muscle cells

Total words: 6860
Number of Figures: 5
Number of Tables: 2

TOC category: Basic
TOC subcategory: Vascular Biology

Abstract

Objective: Recent evidence suggests an important role for angiotensin-converting enzyme 2 (ACE2) in limiting abdominal aortic aneurysm (AAA). This study examined the effect of ACE2 deficiency on AAA development and the efficacy of resveratrol to up-regulate ACE2 in experimental AAA.

Approach and Results: Ace2 deletion in apolipoprotein-deficient mice (*ApoE*$^{-/-}$*Ace2*$^{-/y}$) resulted in increased aortic diameter and spontaneous aneurysm of the suprarenal aorta (SRA) associated with increased expression of inflammation and proteolytic enzyme markers. In humans, serum ACE2 activity was negatively associated with AAA diagnosis. *ACE2* expression was lower in infrarenal biopsies of AAA patients than organ donors. AAA was more severe in *ApoE*$^{-/-}$*Ace2*$^{-/y}$ mice compared to controls in two experimental models. Resveratrol (0.05 g/100 g chow) inhibited growth of pre-established AAAs in *ApoE*$^{-/-}$ mice fed high-fat chow and infused with angiotensin II (AngII) continuously over 56 days. Reduced SRA dilatation in mice receiving resveratrol was associated with elevated serum ACE2, and increased SRA tissue levels of ACE2 and sirtuin (Sirt)1 activity. In addition, the relative phosphorylation of Akt and extracellular signal-regulated kinase 1/2 within SRA tissue, and gene expression for nuclear factor of kappa light polypeptide gene enhancer in B cells 1, angiotensin type-1 receptor, and metallopeptidase 2 and 9 were significantly reduced. Up-regulation of ACE2 in human aortic smooth muscle cells by resveratrol *in vitro* was Sirt1-dependent.

Conclusion: This study provides experimental evidence of an important role for ACE2 in limiting AAA development and growth. Resveratrol upregulated ACE2 and inhibited AAA growth in a mouse model.

Abbreviations	
AAA	abdominal aortic aneurysm
ACE2	angiotensin-converting enzyme 2 (gene = *ACE2* (human); *Ace2* (mouse))
Agtr1	angiotensin type-1 receptor (gene = *AGTR1* (human); *Agtr1* (mouse)
AngII	angiotensin II
AoSMC	human aortic smooth muscle cell
ApoE$^{-/-}$	apolipoprotein E-deficient mouse
ApoE$^{-/-}$*Ace2*$^{-/y}$	whole-body *Ace2*-deficient *ApoE*$^{-/-}$ mouse
IRA	infrarenal aorta
RSV	resveratrol
Sirt1	sirtuin 1 (gene = *SIRT1* (human); *Sirt1* (mouse))
SRA	suprarenal aorta

Introduction

Abdominal aortic aneurysm (AAA) is an important cause of sudden death due to aortic rupture and responsible for ~200,000 deaths worldwide each year [1]. Most AAAs are identified at an early stage when a medical therapy could be instigated to limit AAA progression. There is great interest in identifying targets for the development of drug therapy that can effectively limit AAA growth and aortic rupture as no proven medical treatment is currently available [2,3,4].

Chronic aortic inflammation is thought to play a significant role in AAA pathogenesis through multiple mechanisms including the release of proteolytic enzymes from infiltrating leukocytes, and the generation of reactive oxygen species (ROS) that induce an inflammatory phenotype in vascular smooth muscle cells [5]. The renin-angiotensin-system (RAS) has long been implicated in human AAA pathogenesis [4,5]. Angiotensin II (AngII), the primary effector of the RAS, stimulates pro-inflammatory activity in the vascular wall [6]. Historically, angiotensin-converting enzyme (ACE) and the angiotensin type-1 receptor have been the focus for clinical interventions targeting the RAS, however, recent studies have demonstrated the importance of angiotensin-converting enzyme 2 (ACE2) in maintaining the balance of the RAS [7]. The action of ACE2 to metabolise AngII to vascular-protective peptides such as angiotensin-1-7 (Ang(1-7)) has identified ACE2 as an important negative regulator of the RAS [8,9].

Reduced ACE2 expression has been associated with cardiovascular disease in humans and experimental models [7,10] and therapeutic strategies for augmenting ACE2 expression and activity are thus being developed [11-15]. Previous studies have reported that the 3,5,4´-trihydroxy-*trans*-stilbene resveratrol inhibits experimental aortic aneurysm and dissection development [16-18]. Resveratrol is reported to up-regulate adipose expression of *Ace2* in hyperlipidemic mice [19]. Many of the beneficial cardiovascular properties attributed to resveratrol are believed to be mediated either directly or indirectly through activation of the nicotinamide adenine dinucleotide (NAD^+)-dependent deacetylase sirtuin-1 (Sirt1) [20-22]. Moreover, it has recently been reported that increased ACE2 expression under conditions of cell stress *in vitro* is controlled by Sirt1 [23]. Sirt1 exerts protective effects on a number of cellular processes such as gene regulation, the stress response, apoptosis, inflammation and senescence [24], which are processes implicated in AAA [5,25,26].

The present study investigated the regulatory role of ACE2 in AAA by assessing its genetic deletion, firstly, in otherwise unmanipulated apolipoprotein E-deficient (*ApoE*$^{-/-}$) mice, and then in two mouse models of AAA. ACE2 expression was examined in human serum and aortic tissue samples from AAA patients and controls. Finally, the efficacy of resveratrol in upregulating ACE2 and limiting AAA growth was investigated in a mouse model of established AAA and within *in vitro* studies using human aortic smooth muscle cells (AoSMC).

Material and Methods

Materials and Methods are available in the online-only Data Supplement.

Results

Ace2-deficient *ApoE*$^{-/-}$ mice were predisposed to AAA development and aortic rupture

We examined the suprarenal aorta (SRA) and serum of otherwise unmanipulated *ApoE*$^{-/-}$ mice deficient in Ace2 (*ApoE*$^{-/-}$*Ace2*$^{-/y}$) and age and sex-matched *ApoE*$^{-/-}$ controls. Median maximum diameter of the SRA in *ApoE*$^{-/-}$*Ace2*$^{-/y}$ mice was significantly larger than that in control mice (Figure 1A). Intriguingly, two of the *Ace2*-deficient animals (but none of the controls) exhibited unexpected marked dilatation of the SRA (Figure 1B). Aortic tissue levels of AngII were greater in *ApoE*$^{-/-}$*Ace2*$^{-/y}$ mice compared to *ApoE*$^{-/-}$ controls (22±5 pg/mg protein vs 10±2 pg/mg, respectively; n=6, P<0.001). *ApoE*$^{-/-}$*Ace2*$^{-/y}$ mice exhibited markedly upregulated aortic gene expression for the pro-inflammatory markers interleukin-6, tumour necrosis factor-α, monocyte chemotactic protein-1, vascular cell adhesion molecule-1, and Mac-1/CD11b (Supplementary Figure I). Aortic gene expression for the extracellular matrix proteins collagen I and III, elastin, fibronectin, connective tissue growth factor (CTGF) and transforming growth factor beta (TGFβ) was similar in *ApoE*$^{-/-}$*Ace2*$^{-/y}$ and *ApoE*$^{-/-}$ mice (Supplementary Table I). Aortic gene expression for osteopontin, osteoprotegerin, matrix metallopeptidase (*Mmp*)*2* and *Mmp9* was significantly greater in *ApoE*$^{-/-}$*Ace2*$^{-/y}$ than *ApoE*$^{-/-}$ mice (Supplementary Figure I). Lysyl oxidase activity within aortas of *ApoE*$^{-/-}$*Ace2*$^{-/y}$ mice was down-regulated compared to *ApoE*$^{-/-}$ controls (7.1 ± 0.5 relative fluorescence units (RFU)/ug protein vs 12.8 ± 2.8 RFU/ug protein, respectively; n=8, P=0.025). Serum concentration of AngII was significantly higher in *ApoE*$^{-/-}$*Ace2*$^{-/y}$ mice compared to *ApoE*$^{-/-}$ controls (268±31 pg/ml vs 135±21 pg/ml, respectively; n=6, P<0.001), while serum total cholesterol (10.3±0.6 mM vs 10.1±0.5 mM) and triglyceride (1.1±0.1 mM vs 1.1±0.2 mM) concentrations were comparable. Systolic blood pressure was significantly higher in *ApoE*$^{-/-}$*Ace2*$^{-/y}$ mice compared to controls (110±2 mmHg vs 98±2 mmHg, respectively; n=8, P<0.001).

The effect of *Ace2* deficiency was examined in two models of experimental AAA. Remarkably, subcutaneous infusion of AngII (1μg/kg/min) resulted in an 83% rupture rate (10 out of 12 mice) in *ApoE*$^{-/-}$*Ace2*$^{-/y}$ mice within 7 days of pump insertion, compared to only 15% (2 of the 13) in *ApoE*$^{-/-}$ controls over the 28-day AngII infusion period (Figure 1C & 1D; Supplementary Figure II). *Ace2* deficiency resulted in more severe aortic dilatation within the calcium chloride ($CaCl_2$) model. After $CaCl_2$ application, a time-dependent increase in infrarenal aortic (IRA) diameter was observed by ultrasound in both *ApoE*$^{-/-}$ (P<0.001, ANOVA) and *ApoE*$^{-/-}$*Ace2*$^{-/y}$ (P<0.001, ANOVA) mice (Figure 1E). The rate of IRA expansion was markedly greater in *ApoE*$^{-/-}$*Ace2*$^{-/y}$ than control mice (P=0.034, linear mixed-effects (LME); Figure 1E). There were no aortic ruptures in either group of mice within the $CaCl_2$ model. At the end of the study the aortas were harvested from all mice and used to perform morphometric analyses. A markedly greater percent-increase in IRA diameter (relative to corresponding sham controls) was demonstrated in *ApoE*$^{-/-}$*Ace2*$^{-/y}$ mice compared to *ApoE*$^{-/-}$ controls (Figure 1F; Supplementary Figure III).

Serum ACE2 activity and aortic expression of ACE2 were reduced in AAA patients

ACE2 activity was measured in serum samples obtained from 548 participants of the *Health In Men Study* (HIMS), comprising 205 men who had an AAA and 343 who did not. Participant demographic characteristics are presented in Supplementary Table II. The association of circulating ACE2 activity with AAA diagnosis was assessed

using binary logistic regression including analyses which adjusted for established AAA risk factors (Supplementary Table III). ACE2 activity had a significant inverse association with AAA diagnosis after adjusting for AAA risk factors and potential confounders (P=0.032; Supplementary Table III). A similar trend was observed in the unadjusted analysis although the association was not statistically significant (P=0.087).

Expression of *ACE* and *ACE2,* and the level of CpG island methylation in the promoter region of *ACE2* (Supplementary Figure IV) were assessed in infrarenal aortic biopsies collected from patients undergoing open surgery for AAA repair and from heart-beating brain dead organ donors (controls). Demographic characteristics of the participants are presented in Supplementary Table IV. Expression of *ACE* was similar in AAA and control biopsies (Supplementary Figure V), however *ACE2* was down-regulated 8-fold in AAA biopsies compared to controls (P=0.024; Supplementary Figure V). Hyper-methylation of 12 CpG sites was found in all AAA samples and the mean percentage CpG island methylation was higher in AAA than control aortic biopsies (P=0.032; Supplementary Figure VI).

Growth of pre-induced AAAs was inhibited with dietary resveratrol supplementation in a mouse model

Two consecutive 28-day subcutaneous pumps were implanted (day 0 and day 29) in a cohort of high-fat chow (HFC)-fed *ApoE*$^{-/-}$ mice to supply continuous AngII (1.0 µg/kg/min) over an eight-week experimental period (Supplementary Figure VII). After an initial 14-day AAA establishment period, surviving mice were allocated to receive either HFC (control; n=15) or HFC + 0.05 g resveratrol/100 g HFC (intervention; n=15) diets for the remaining six weeks.

Continuous AngII infusion during the intervention period resulted in a mortality rate due to aortic rupture of 27% (4 out of 15) in the control (HFC) group versus 7% (1 out of 15) in the intervention (HFC + resveratrol) group (Supplementary Figure VIII). The reduced rupture rate in mice receiving resveratrol was not statistically significant (P=0.130, Log-rank test; Supplementary Figure VIII). Body-weight of surviving mice fed either HFC (P<0.001, ANOVA) or resveratrol-supplemented HFC (P<0.001, ANOVA) diets increased over the six-week intervention period (Figure 2A). However, the rate of increase in bodyweight was markedly reduced in mice receiving resveratrol (P<0.001, LME; Figure 2A). The average amount of food consumed over the experimental period was comparable between the groups (Supplementary Figure IX).

A time-dependent increase in maximum SRA diameter in response to AngII was observed by ultrasound in control mice over the six-week period (P<0.001, ANOVA; Figure 2B). In contrast, the maximum SRA diameter in mice administered HFC diet supplemented with resveratrol did not change significantly (P=0.318, ANOVA; Figure 2B). Control mice exhibited a substantially greater rate of SRA expansion over the intervention period compared to mice receiving resveratrol (P=0.034, LME; Figure 2B). Mice receiving resveratrol that reached the end of the experimental period had significantly smaller maximum SRA diameter than controls when measured by morphometry (P<0.001; Figure 2C; Supplementary Figure X).

Serum concentration of ACE2 was determined in all mice at baseline, at the time of allocation to the interventional and control groups (day 14), and at the completion of the intervention period. A decrease in serum ACE2 concentration over time was demonstrated in control mice in response to AngII infusion and HFC diet (P=0.026, ANOVA; Figure 2D). At the end of the study (day 56), the median serum concentration of ACE2 in these mice was significantly lower than at baseline (P=0.015; Figure 2D). Supplementation of the HFC diet with resveratrol inhibited the reduction in

serum ACE2 concentration (P=0.075 compared to baseline, ANOVA; Figure 2D), and median concentration of serum ACE2 in mice receiving resveratrol was above baseline and 4-fold higher than in control mice at the end of the study (P=0.005; Figure 2D).

Ace2 gene expression and protein concentration within the SRA was greater in mice receiving resveratrol than controls (Table 1; Figure 2E). *Sirt1* expression and Sirt1 deacetylase activity within the SRA was markedly greater in mice receiving resveratrol compared to controls (Table 1; Figure 2F). Protein concentration of total protein kinase B (Akt1) and extracellular signal-regulated kinase (ERK)1/2 kinases within the SRA tissue of mice receiving resveratrol were similar to concentrations in control mice (Supplementary Figure XI). The ratio of phosphorylated-to-total kinase (activity) for both Akt1 and ERK1/2 within SRA tissue from mice receiving resveratrol was significantly lower than that within SRA tissue from mice on the control diet (Figure 3). Gene expression for the inflammatory marker nuclear factor of kappa light polypeptide gene enhancer in B cells 1 (*Nfkb1*) and proteolytic enzymes *Mmp2* and *Mmp9* within the SRA of mice receiving resveratrol was down-regulated 4.5-, 3-, and 2-fold, respectively, compared to controls, while gene expression for the angiotensin II type-1 receptor (*Agtr1*) was 2-fold lower in mice receiving resveratrol compared to controls (Table 1).

Normalisation of *ACE2* in inflammation-activated human AoSMC via resveratrol-mediated Sirt1 activation

The effect of resveratrol (5 μM) on resting human AoSMC, and *inflammation-activated* AoSMC was examined *in vitro*. The expression of *NFKB1*, *AGTR1*, *ACE2,* and *SIRT1* genes in resting AoSMC is shown in Table 2. While no significant change in basal expression of *NFKB1* was seen, incubation of cells with resveratrol over 24 hours resulted in a significant decrease in *AGTR1* and increases in *ACE2* and *SIRT1* expression (Table 2).

Cell stress was modelled in AoSMC via exposure to activated monocyte-derived pro-inflammatory media over five days. Control cells incubated in pro-inflammatory media alone exhibited marked increases in the expression of *NFKB1* and *AGTR1*, with significant down-regulation of *ACE2* and *SIRT1* (Figure 4A-D). The reduction in *ACE2* and *SIRT1* gene expression correlated with significant reduction in cellular protein and cellular activity of ACE2 and Sirt1, respectively (Figure 4E&F). Supplementation of the pro-inflammatory media with 5 μM resveratrol during the final 24 hours of the five-day incubation resulted in changes in expression for all four genes to within baseline expression ranges (Figure 4A-D). Notably, cellular ACE2 protein and Sirt1 activity were upregulated and measured at levels significantly higher than baseline (Figure 4E&F).

The positive effect of resveratrol on gene and protein expression of ACE2 was ablated upon targeted knock-down of Sirt1 (Figure 5). Gene silencing of *SIRT1* in activated AoSMC performed using small interfering (si) RNA added after 36 hours incubation in pro-inflammatory media resulted in 2-fold down-regulation in *SIRT1* expression (P=0.002; Figure 5A). Supplementation with 5 μM resveratrol 24 hours following *SIRT1* silencing failed to correct down-regulated *ACE2* expression or cellular ACE2 protein levels (Figure 5B&C).

Discussion

The main finding of this study was that dietary resveratrol supplementation significantly inhibited progression of AAA in a mouse model. The effect of resveratrol was associated with up-regulation of ACE2 expression and Sirt1 activity within the aorta. A link between resveratrol-mediated up-regulation of ACE2 and increased Sirt1 activity was demonstrated in human AoSMC *in vitro*.

Preclinical and clinical studies have demonstrated that ACE2 deficiency promotes susceptibility to metabolic and cardiovascular disease [7], however the importance of ACE2 in AAA has only recently received attention [13,15,27]. Thatcher *et al* [13] first reported that *Ace2* deficiency in low-density lipoprotein receptor-deficient mice promoted dilatation of the SRA in response AngII infusion. The current study supports and extends these finding by reporting increased propensity to AAA development by *ApoE*$^{-/-}$*Ace2*$^{-/y}$ mice when AAA is induced by either AngII or $CaCl_2$. Notable was the presence of larger SRA diameter and spontaneous aneurysm in otherwise unmanipulated *ApoE*$^{-/-}$*Ace2*$^{-/y}$ mice. We and others have reported that *Ace2* deficiency predisposes to vascular inflammation in the *ApoE*$^{-/-}$ mouse [27,28] and results in increased circulating and tissue levels of AngII [28,29]. Higher concentration of AngII and increased markers of extracellular matrix inflammation and degeneration within aortic tissue of *ApoE*$^{-/-}$*Ace2*$^{-/y}$ mice was confirmed in the current study. While there appeared to be no change in collagen synthesis or in the expression of pro-fibrotic mediators like TGFβ and CTGF, proteolytic enzymes MMP2 and MMP9 were up-regulated and LOX activity decreased in *ApoE*$^{-/-}$*Ace2*$^{-/y}$ mice. LOX is an extracellular copper enzyme that initiates crosslinking of collagen and elastin to provide vascular tensile strength and elasticity, and its deficiency leads to aneurysm formation and premature death in mice [30,31]. Aortic expression of osteoprotegerin, a protein that we and others have shown to promote AAA through stimulating protease release from monocytes and vascular smooth muscle cells [32,33], was increased also in *ApoE*$^{-/-}$*Ace2*$^{-/y}$ mice compared to *ApoE*$^{-/-}$ controls. It is highly likely that these pre-existing differences in expression for markers of inflammation and extracellular matrix turnover, AngII concentration and blood pressure, accounted for the increased SRA dilatation in *ApoE*$^{-/-}$*Ace2*$^{-/y}$ mice, and predisposed these mice to more severe AngII or $CaCl_2$-induced aortic aneurysms compared to controls.

Previous investigation of ACE2 in human AAA patients has been limited. Previous studies that measured plasma or serum ACE2 indicate that circulating ACE2 activity is low in healthy subjects, comparably increased in subjects with cardiovascular risk factors, and correlated with cardiovascular disease development [34,35]. Here, we measured serum ACE2 activity in men that did and did not have ultrasound screeningdetected AAAs and found relative lower levels in men with an AAA after adjusting for other risk factors. This appears in contrast with existing published data on circulating ACE2 and cardiovascular disease. Importantly, ACE2 undergoes cleavage (‘shedding’) to release the catalytically active ectodomain into the extracellular milieu and circulation [36], however whether the degree of ACE2 activity within the circulation correlates with tissue ACE2 synthesis and/or ACE2 shedding from tissue remains uncertain and requires further investigation. We also found the hyper-methylation of the *ACE2* promoter and down-regulation of *ACE2* expression in human AAA biopsies compared to samples from donor controls. Overall these findings suggest down-regulation of ACE2 in AAA patients. Interestingly, low serum ACE2 was recently reported as an independent risk factor and potential prognostic for in-hospital mortality following open repair of ruptured AAA [37].

The ACE2/Ang(1-7)/mas receptor axis has emerged within the RAS as a counterbalance to the classical ACE/AngII/AT1R pathway [8,9], and, subsequently, ACE2 as a potential therapeutic target for the treatment of cardiovascular diseases [7,38]. Pre-clinically, therapeutic strategies for ACE2 involve augmenting its activity or expression. To this end, adenovirus-mediated *Ace2* gene transfer [15] and ACE2 activation (diminazene aceturate) [13] have been utilised in mouse models of AAA with promising outcomes. The current study adopted an alternative approach. The natural dietary 3,5,4´-trihydroxy-*trans*-stilbene resveratrol has been reported to inhibit AAA development in several rodent models [16-18], and in an unrelated study, increase fat tissue *Ace2* expression in mice [19]. We investigated the efficacy of resveratrol to positively regulate aortic *Ace2* expression, and limit growth of established AAA in a mouse model.

Resveratrol administration increased SRA and serum levels of ACE2. The up-regulation of ACE2 in the SRA of mice receiving resveratrol was associated with concomitant increase in mRNA and activity for Sirt1. Sirt1 is a NAD^+-dependent protein deacetylase highly expressed in the vasculature [39]. An increasing number of vascular-protective actions for Sirt1, including modulation of stress-induced vascular remodelling, are being recognised [40,41]. Very recent studies suggest that reduced Sirt1 production and activity in vascular smooth muscle links vascular senescence and inflammation to AAA [42]. Sirt1 is a putative target for resveratrol with direct and indirect mechanisms described for resveratrol activation of Sirt1 [20-22]. Up-regulation of *ACE2* expression by Sirt1 under conditions of energy stress has recently been reported [23] and is of particular relevance to the current study. We demonstrated in an *in vitro* model of inflammation the down-regulation of both ACE2 and Sirt1 in human AoSMC. More important was that rescue and up-regulation of ACE2 in these cells by resveratrol was abolished upon pre-incubation of AoSMC with Sirt1-targeted siRNA, thus establishing a potential dependant link between resveratrol, Sirt1 activation, and positive regulation of vascular ACE2.

The relative levels of phosphorylated Akt and ERK1/2 within the SRA of *ApoE*$^{-/-}$ mice have been previously reported to be increased following AngII-infusion [43]. The Akt and ERK1/2 pathways have been implicated in the activation of extracellular remodelling enzymes and inflammation in AAA [44,45]. Notably, ACE2 deficiency has been reported to promote AngII-mediated aortic inflammation and oxidative stress associated with the activation of Akt/ERK/eNOS signaling [46]. Resveratrol has been reported to inhibit ROS overproduction in vascular smooth muscle through suppression of Akt and p38 MAPK/JNK/ERK phosphorylation [47]. In the current study, we found marked reduction in the relative levels of phosphorylated Akt and ERK1/2 within SRA samples of mice receiving resveratrol. This finding suggests that resveratrol administration led to down-regulation of both the Akt and ERK1/2 signaling pathways. Aortic expression of *Nfkb1*, *Mmp2*, *Mmp9,* and *Agtr1*, were also downregulated in mice receiving resveratrol suggesting that the abovementioned effect of resveratrol resulted in less aortic inflammation and expression of matrix degrading enzymes.

A number of study limitations are acknowledged. First, sample numbers for the human infrarenal aortic tissue study were relatively small. As most AAAs are now managed by endovascular repair, AAA wall biopsies are increasingly difficult to obtain. Similarly, ethical and practical considerations prevent the collection of aortic biopsies from large numbers of control donors; however, sample sizes were similar to other published studies [25,48,49]. Second, the organ donor controls were younger than the patients with AAA, and the possibility that the age discrepancy may have contributed to differences in *ACE2* expression is recognised. Limited clinical details were available

for the organ donor controls and variation in cardiovascular risk factors between groups could not be adjusted for. However, organ donors are often the only viable source of healthy aortic biopsies. Previous studies have utilized macroscopically healthy tissues proximal to the AAA sac as matched control tissues [50,51]; but these were not available for the current study. Third, we did not conclusively demonstrate that the benefits of resveratrol to limit AAA growth resulted from ACE2 upregulation. Ideally a study of the effect of resveratrol in *ApoE*$^{-/-}$*Ace2*$^{-/y}$ mice and *ApoE*$^{-/-}$ controls would have been performed but was not feasible due to the substantial aortic rupture rate in *ApoE*$^{-/-}$*Ace2*$^{-/y}$ mice in response to AngII. Finally, *in vitro* studies were conducted only in AoSMC. We acknowledge that resveratrol has been shown to improve endothelial function and increased expression of ACE2 has been reported to promote positive endothelial responses to inflammation [52,53]. It is therefore possible that the beneficial effects of resveratrol may have been due to effects on endothelial or even inflammatory cells. However the current study focused on progression of *established* AAA. A recognised feature of AAA progression in humans is phenotypic change, accelerated replicative senescence, apoptosis, and subsequent depletion of medial AoSMC [26,54]. This and recent evidence that ACE2 deficiency in AoSMC markedly increases ROS and apoptosis in response to AngII [27] formed the basis for the rationale to focus *in vitro* studies on AoSMC.

In summary, the current study provides further experimental evidence of an important role for ACE2 in vascular homeostasis and as a modulator of AAA severity. Dietary administration of resveratrol upregulated ACE2 and inhibited AAA progression in a mouse model. The up-regulation of aortic ACE2 was paralleled by increased expression and activity of Sirt1, and down-regulation of key signaling pathways and markers of inflammation. Resveratrol rescued AoSMC expression and production of ACE2 in a Sirt1-dependent manner *in vitro*.

Acknowledgements

None.

Sources of Funding

This work was supported by the National Health and Medical Research Council (grants 1079193, 1079369 and 1098717, Practitioner Fellowship 1117061), the Office of Health and Medical Research, the Townsville Hospital Private Practice Trust and Queensland Government. The funding bodies played no role in generation of the data presented in this publication.

Disclosures

All the authors have no conflicts of interest or financial ties to disclose.

References

1. Sampson UK, Norman PE, Fowkes FG, Aboyans V, Yanna Song, Harrell FE Jr, Forouzanfar MH, Naghavi M, Denenberg JO, McDermott MM, Criqui MH, Mensah GA, Ezzati M, Murray C. Global and regional burden of aortic dissection and aneurysms: mortality trends in 21 world regions, 1990 to 2010. Glob Heart 2014;9:171-180.
2. Golledge J, Norman PE. Current status of medical management for abdominal aortic aneurysm. Atherosclerosis 2011;217:57-63.
3. Rughani G, Robertson L, Clarke M. Medical treatment for small abdominal aortic aneurysms. Cochrane Database Syst Rev 2012;9:CD009536.
4. Golledge J, Norman PE, Murphy MP, Dalman RL. Challenges and opportunities in limiting abdominal aortic aneurysm growth. J Vasc Surg 2017;65:225-233.
5. Golledge J, Muller J, Daugherty A, Norman P. Abdominal aortic aneurysm: pathogenesis and implications for management. Arterioscler Thromb Vasc Biol 2006;26:2605-2613.
6. Ejiri J, Inoue N, Tsukube T, Munezane T, Hino Y, Kobayashi S, Hirata K, Kawashima S, Imajoh-Ohmi S, Hayashi Y, Yokozaki H, Okita Y, Yokoyama M. Oxidative stress in the pathogenesis of thoracic aortic aneurysm: protective role of statin and angiotensin II type 1 receptor blocker. Cardiovasc Res 2003;59:988-996.
7. Tikellis C, Thomas MC. Angiotensin-Converting Enzyme 2 (ACE2) is a key modulator of the renin angiotensin system in health and disease. Int J Pept 2012;2012:256294.
8. Burrell LM, Johnston CI, Tikellis C, Cooper ME. ACE2, a new regulator of the renin-angiotensin system. Trends Endocrinol Metab 2004;15:166-169.
9. Chappel MC, Ferrario CM. ACE and ACE2: their role to balance the expression of angiotensin II and angiotensin-(1–7). Kidney Int 2006;70:8-10.
10. Burrell LM, Harrap SB, Velkoska E, Patel SK. The ACE2 gene: its potential as a functional candidate for cardiovascular disease. Clin Sci (Lond) 2013;124:65-76.
11. Rentzsch B, Todiras M, Iliescu R, Popova E, Campos LA, Oliveira ML, Baltatu OC, Santos RA, Bader M. Transgenic angiotensin-converting enzyme 2 overexpression in vessels of SHRSP rats reduces blood pressure and improves endothelial function. Hypertension 2008;52:967-73.
12. Zhang C, Zhao YX, Zhang YH, Zhu L, Deng BP, Zhou ZL, Li SY, Lu XT, Song LL, Lei XM, Tang WB, Wang N, Pan CM, Song HD, Liu CX, Dong B, Zhang Y, Cao Y. Angiotensin-converting enzyme 2 attenuates atherosclerotic lesions by targeting vascular cells. Proc Natl Acad Sci USA 2010;107:15886-91.
13. Thatcher SE, Zhang X, Howatt DA, Yiannikouris F, Gurley SB, Ennis T, Curci JA, Daugherty A, Cassis LA. Angiotensin-converting enzyme 2 decreases formation and severity of angiotensin II-induced abdominal aortic aneurysms. Arterioscler Thromb Vasc Biol 2014;34:2617-2623.
14. Singh N, Joshi S, Guo L, Baker MB, Li Y, Castellano RK, Raizada MK, Jarajapu YP. ACE2/Ang-(1-7)/Mas axis stimulates vascular repair-relevant functions of CD34+ cells. Am J Physiol Heart Circ Physiol 2015;309:H1697-707.
15. Hao Q, Dong X, Chen X, Yan F, Wang X, Shi H, Dong B. ACE2 Inhibits Angiotensin II-Induced Abdominal Aortic Aneurysm in Mice. Hum Gene Ther 2017 Jan 31 [Epub ahead of print].
16. Kaneko H, Anzai T, Morisawa M, Kohno T, Nagai T, Anzai A, Takahashi T, Shimoda M, Sasaki A, Maekawa Y, Yoshimura K, Aoki H, Tsubota K, Yoshikawa

T, Okada Y, Ogawa S, Fukuda K. Resveratrol prevents the development of abdominal aortic aneurysm through attenuation of inflammation, oxidative stress, and neovascularization. Atherosclerosis 2011;217:350-357.
17. Palmieri D, Pane B, Barisione C, Spinella G, Garibaldi S, Ghigliotti G, Brunelli C, Fulcheri E, Palombo D. Resveratrol counteracts systemic and local inflammation involved in early abdominal aortic aneurysm development. J Surg Res 2011;171:e237-246.
18. Hibender S, Franken R, van Roomen C, Ter Braake A, van der Made I, Schermer EE, Gunst Q, van den Hoff MJ, Lutgens E, Pinto YM, Groenink M, Zwinderman AH, Mulder BJ, de Vries CJ, de Waard V. Resveratrol Inhibits Aortic Root Dilatation in the Fbn1C1039G/+ Marfan Mouse Model. Arterioscler Thromb Vasc Biol 2016;36:1618-1626.
19. Oliveira Andrade JM, Paraíso AF, Garcia ZM, Ferreira AV, Sinisterra RD, Sousa FB, Guimarães AL, de Paula AM, Campagnole-Santos MJ, dos Santos RA, Santos SH. Cross talk between angiotensin-(1-7)/Mas axis and sirtuins in adipose tissue and metabolism of high-fat feed mice. Peptides 2014;55:158-165.
20. Bonnefont-Rousselot D. Resveratrol and cardiovascular diseases. Nutrients 2016;8:250.
21. Zordoky BN, Robertson IM, Dyck JR. Preclinical and clinical evidence for the role of resveratrol in the treatment of cardiovascular diseases. Biochim Biophys Acta 2015;1852:1155-77.
22. Park SJ, Ahmad F, Philp A, Baar K, Williams T, Luo H, Ke H, Rehmann H, Taussig R, Brown AL, Kim MK, Beaven MA, Burgin AB, Manganiello V, Chung JH. Resveratrol ameliorates aging-related metabolic phenotypes by inhibiting cAMP phosphodiesterases. Cell 2012;148:421-433.
23. Clarke NE, Belyaev ND, Lambert DW, Turner AJ. Epigenetic regulation of angiotensin-converting enzyme 2 (ACE2) by SIRT1 under conditions of cell energy stress. Clin Sci (Lond) 2014;126:507-516.
24. Alcendor RR, Gao S, Zhai P, Zablocki D, Holle E, Yu X, Tian B, Wagner T, Vatner SF, Sadoshima J. Sirt1 regulates aging and resistance to oxidative stress in the heart. Circ Res 2007;100:1512–1521.
25. Biros E, Gäbel G, Moran CS, Schreurs C, Lindeman JH, Walker PJ, Nataatmadja M, West M, Holdt LM, Hinterseher I, Pilarsky C, Golledge J. Differential gene expression in human abdominal aortic aneurysm and aortic occlusive disease. Oncotarget 2015;6:12984-96.
26. Liao S, Curci JA, Kelley BJ, Sicard GA, Thompson RW. Accelerated replicative senescence of medial smooth muscle cells derived from abdominal aortic aneurysms compared to the adjacent inferior mesenteric artery. J Surg Res 2000;92:85-95.
27. Patel VB, Zhong JC, Fan D, Basu R, Morton JS, Parajuli N, McMurtry MS, Davidge ST, Kassiri Z, Oudit GY. Angiotensin-converting enzyme 2 is a critical determinant of angiotensin II-induced loss of vascular smooth muscle cells and adverse vascular remodeling. Hypertension 2014;64:157-164.
28. Thomas MC, Pickering RJ, Tsorotes D, Koitka A, Sheehy K, Bernardi S, Toffoli B, Nguyen-Huu TP, Head GA, Fu Y, Chin-Dusting J, Cooper ME, Tikellis C. Genetic Ace2 deficiency accentuates vascular inflammation and atherosclerosis in the ApoE knockout mouse. Circ Res 2010;107:888-897.
29. Tikellis C, Bialkowski K, Pete J, Sheehy K, Su Q, Johnston C, Cooper ME, Thomas MC. ACE2 deficiency modifies renoprotection afforded by ACE inhibition in experimental diabetes. Diabetes 2008;57:1018-1025.

30. Mäki JM, Räsänen J, Tikkanen H, Sormunen R, Mäkikallio K, Kivirikko KI, Soininen R. Inactivation of the lysyl oxidase gene Lox leads to aortic aneurysms, cardiovascular dysfunction, and perinatal death in mice. Circulation 2002;106:2503-2509.
31. Krishna SM, Seto SW, Jose RJ, Biros E, Moran CS, Wang Y, Clancy P, Golledge J. A peptide antagonist of thrombospondin-1 promotes abdominal aortic aneurysm progression in the angiotensin II-infused apolipoprotein-E-deficient mouse. Arterioscler Thromb Vasc Biol 2015;35:389-398.
32. Moran CS, Jose RJ, Biros E, Golledge J. Osteoprotegerin deficiency limits angiotensin II-induced aortic dilatation and rupture in the apolipoprotein E-knockout mouse. Arterioscler Thromb Vasc Biol 2014;34:2609-2616.
33. Koole D, Hurks R, Schoneveld A, Vink A, Golledge J, Moran CS, de Kleijn DP, van Herwaarden JA, de Vries JP, Laman JD, Huizinga R, Pasterkamp G, Moll FL. Osteoprotegerin is associated with aneurysm diameter and proteolysis in abdominal aortic aneurysm disease. Arterioscler Thromb Vasc Biol 2012;32:1497-1504.
34. Patel SK, Velkoska E, Burrell LM. Emerging markers in cardiovascular disease: where does angiotensin-converting enzyme 2 fit in? Clin Exp Pharmacol Physiol 2013;40:551-559.
35. Úri K, Fagyas M, Kertész A, Borbély A, Jenei C, Bene O, Csanádi Z, Paulus WJ, Édes I, Papp Z, Tóth A, Lizanecz E. Circulating ACE2 activity correlates with cardiovascular disease development. J Renin Angiotensin Aldosterone Syst 2016;17:pii.
36. Lew RA, Warner FJ, Hanchapola I, Yarski MA, Ramchand J, Burrell LM, Smith AI. Angiotensin-converting enzyme 2 catalytic activity in human plasma is masked by an endogenous inhibitor. Exp Physiol 2008;93:685-693.
37. Nie W, Wang Y, Yao K, Wang Z, Wu H. Serum angiotensin-converting enzyme 2 is an independent risk factor for in-hospital mortality following open surgical repair of ruptured abdominal aortic aneurysm. Exp Ther Med 2016;12:1412-1418.
38. Castro-Chaves P, Cerqueira R, Pintalhao M, Leite-Moreira AF. New pathways of the renin-angiotensin system: the role of ACE2 in cardiovascular pathophysiology and therapy. Expert Opin Ther Targets 2010;14:485-496.
39. Potente M, Ghaeni L, Baldessari D, Mostoslavsky R, Rossig L, Dequiedt F, Haendeler J, Mione M, Dejana E, Alt FW, Zeiher AM, Dimmeler S. SIRT1 controls endothelial angiogenic functions during vascular growth. Genes Dev 2007;21:2644-2658.
40. Gao P, Xu TT, Lu J, Li L, Xu J, Hao DL, Chen HZ, Liu DP. Overexpression of SIRT1 in vascular smooth muscle cells attenuates angiotensin II induced vascular remodeling and hypertension in mice. J Mol Med (Berl) 2014;92:347-357.
41. Ma L, Li Y. SIRT1: role in cardiovascular biology. Clin Chim Acta 2015;440:8-15.
42. Chen HZ, Wang F, Gao P, Pei JF, Liu Y, Xu TT, Tang X, Fu WY, Lu J, Yan YF, Wang XM, Han L, Zhang ZQ, Zhang R, Zou MH, Liu DP. Epub 2016 Sep 20. Age-associated Sirtuin 1 reduction in vascular smooth muscle links vascular senescence and inflammation to abdominal aortic aneurysm. Circ Res 2016;119:1076-1088.
43. Zheng YH, Li FD, Tian C, Ren HL, Du J, Li HH. Notch γ-secretase inhibitor dibenzazepine attenuates angiotensin II-induced abdominal aortic aneurysm in ApoE knockout mice by multiple mechanisms. PLoS One 2013;8:e83310.

44. Ghosh A, Lu G, Su G, McEvoy B, Sadiq O, DiMusto PD, Laser A, Futchko JS, Henke PK, Eliason JL, Upchurch GR Jr. Phosphorylation of Akt and Abdominal Aortic Aneurysm. Am J Pathol 2014;184:148-158.
45. Ghosh A, DiMusto PD, Ehrlichman LK, Sadiq O, McEvoy B, Futchko JS, Henke PK, Eliason JL, Upchurch GR Jr. The role of extracellular signal-related kinase during abdominal aortic aneurysm formation. J Am Coll Surg 2012;215:668-680.
46. Jin HY, Song B, Oudit GY, Davidge ST, Yu HM, Jiang YY, Gao PJ, Zhu DL, Ning G, Kassiri Z, Penninger JM, Zhong JC. ACE2 deficiency enhances angiotensin II-mediated aortic profilin-1 expression, inflammation and peroxynitrite production. PLoS One 2012;7:e38502.
47. Guo R, Li W, Liu B, Li S, Zhang B, Xu Y. Resveratrol protects vascular smooth muscle cells against high glucose-induced oxidative stress and cell proliferation in vitro. Med Sci Monit Basic Res 2014;20:82-92.
48. Koole D, van Herwaarden JA, Schalkwijk CG, Lafeber FPJG, Vink A, Smeets MB, Pasterkamp G, Moll FL. A potential role for glycated cross-links in abdominal aortic aneurysm disease. J Vasc Surg 2017;65:1493-1503.
49. Villard C, Eriksson P, Kronqvist M, Lengquist M, Jorns C, Hartman J, Roy J, Hultgren R. Differential expression of sex hormone receptors in abdominal aortic aneurysms. Maturitas. 2017;96:39-44.
50. Emeto TI, Moxon JV, Biros E, Rush CM, Clancy P, Woodward L, et al. Urocortin 2 is associated with abdominal aortic aneurysm and mediates anti-proliferative effects on vascular smooth muscle cells via corticotrophin releasing factor receptor 2. Clin Sci 2014;126:517e27.
51. Biros E, Moran CS, Wang Y, Walker PJ, Cardinal J, Golledge J. microRNA profiling in patients with abdominal aortic aneurysms: the significance of miR-155. Clin Sci 2014;126:795e803.
52. Csiszar A, Labinskyy N, Pinto JT, Ballabh P, Zhang H, Losonczy G, Pearson K, de Cabo R, Pacher P, Zhang C, *et al*. Resveratrol induces mitochondrial biogenesis in endothelial cells. Am J Physiol Heart Circ Physiol 2009;297:H13–H20.
53. Fraga-Silva RA, Costa-Fraga FP, Murça TM, Moraes PL, Martins Lima A, Lautner RQ, Castro CH, Soares CM, Borges CL, Nadu AP, Oliveira ML, Shenoy V, Katovich MJ, Santos RA, Raizada MK, Ferreira AJ. Angiotensin-converting enzyme 2 activation improves endothelial function. Hypertension 2013;61:1233-1238.
54. Ailawadi G, Moehle CW, Pei H, Walton SP, Yang Z, Kron IL, Lau CL, Owens GK. Smooth muscle phenotypic modulation is an early event in aortic aneurysms. J Thorac Cardiovasc Surg 2009;138:1392-1399.

Highlights

- ACE2 deficiency promoted experimental AAA development and rupture
- ACE2 expression was down-regulated in human AAA patients
- Resveratrol inhibited progression of experimental AAA associated with up-regulation of aortic ACE2
- Up-regulation of ACE2 in human AoSMC by resveratrol *in vitro* was Sirt1-dependent

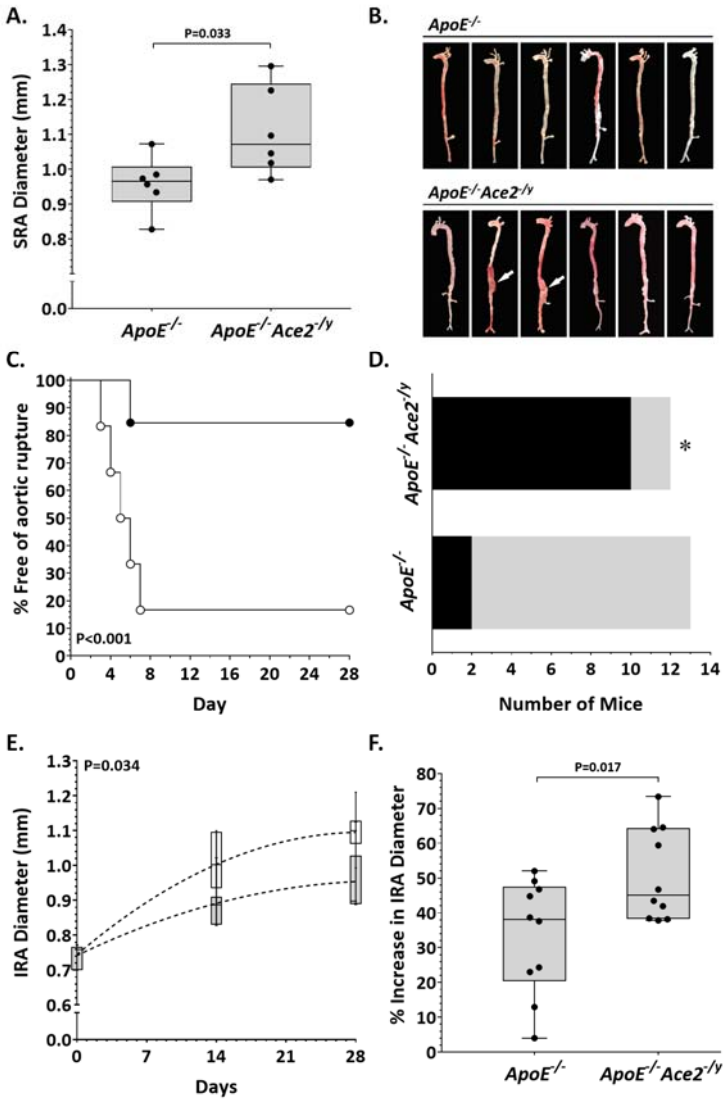

Figure 1: Predisposition of *ApoE*$^{-/-}$*Ace2*$^{-/y}$ mice to aortic dilatation. Larger maximum SRA diameter (**A**) and SRA aneurysms (arrow; **B**) in otherwise unmanipulated *ApoE*$^{-/-}$*Ace2*$^{-/y}$ mice compared to *ApoE*$^{-/-}$ control mice. Data expressed as median and interquartile range with maximum and minimum data points (whiskers) for maximum SRA diameter (mm; **A**). **C.** Kaplan-Meier curves illustrating survival data for AngII-infused *ApoE*$^{-/-}$*Ace2*$^{-/y}$ (open circle) and *ApoE*$^{-/-}$ mice (closed circle); P-value calculated using Log-rank (Mantel-Cox) test. **D.** Incidence of aortic rupture (black) within total number of mice per group (gray); *P=0.001 compared with control by Fisher exact test. **E.** Ultrasound measurement of infra-renal (IRA) dilatation induced by $CaCl_2$ over 28 days in *ApoE*$^{-/-}$*Ace2*$^{-/y}$ (white bar) compared to *ApoE*$^{-/-}$ control mice (grey bar). Data expressed as median and interquartile range with maximum and minimum data points (whiskers) for maximum diameter (mm); P-value calculated for difference between groups by mixed-effects linear regression. **F.** Increase in IRA diameter induced by $CaCl_2$ in *ApoE*$^{-/-}$*Ace2*$^{-/y}$ mice compared to *ApoE*$^{-/-}$ controls. Data expressed as median and interquartile range with maximum and minimum data points (whiskers) for percent increase in diameter relative to sham controls.

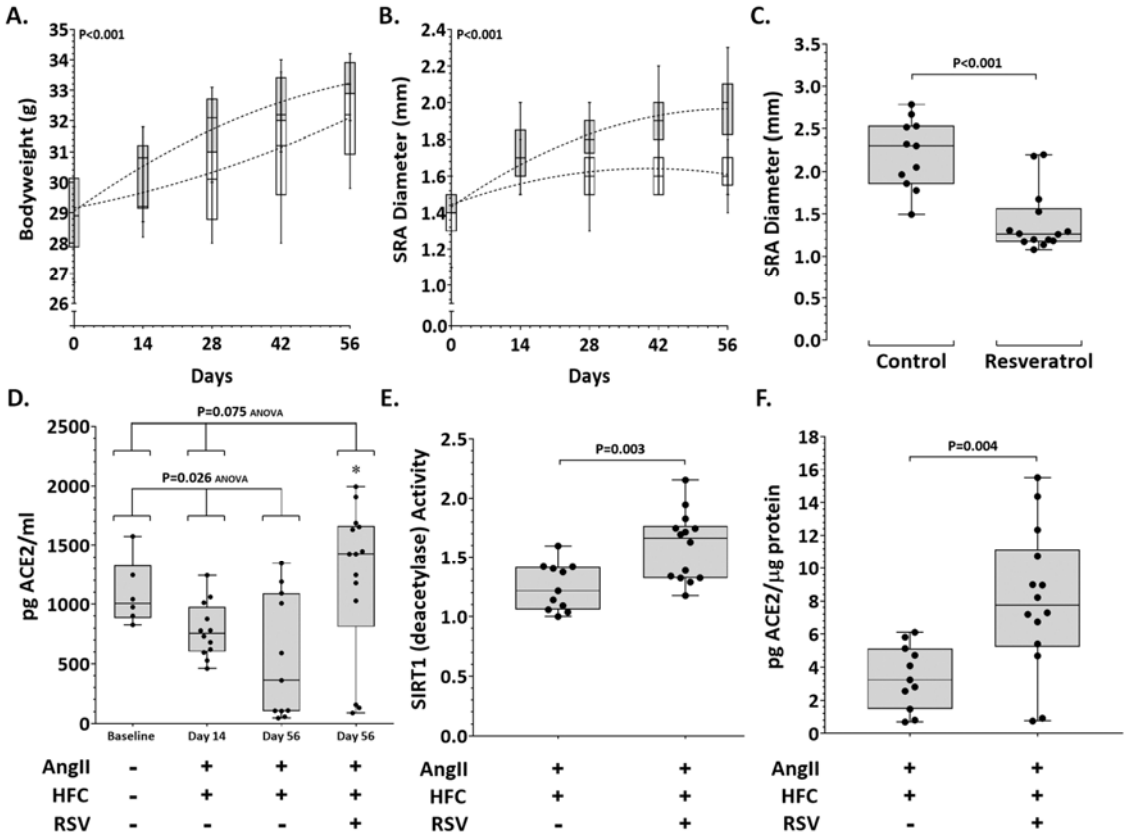

Figure 2: Effect of resveratrol in an AngII-infused, high fat-fed, *ApoE*$^{-/-}$ model of established AAA. Bodyweight (**A**) and ultrasound measurement of the SRA (**B**) in *ApoE*$^{-/-}$ mice receiving high-fat chow (HFC; grey) and HFC + 0.05 g resveratrol/100 g HFC (white). Data expressed as median and interquartile range with maximum and minimum data points (whiskers) for bodyweight (g; **A**) and maximum SRA diameter (mm; **B**); P-values calculated for difference between groups by mixed-effects linear regression. **C.** Maximum SRA diameter at the end of the study in *ApoE*$^{-/-}$ mice receiving control diet (HFC) and resveratrol-supplemented diet (HFC + 0.05 g resveratrol/100 g HFC). Data expressed as median and interquartile range with maximum and minimum data points (whiskers) for diameter (mm). **D.** Serum ACE2 concentration at baseline, 14 days, and 56 days during an AngII infusion in *ApoE*$^{-/-}$ mice receiving HFC, and at day 56 in *ApoE*$^{-/-}$ mice receiving HFC supplemented with resveratrol (RSV). Data expressed as median and interquartile range with maximum and minimum data points (whiskers) for concentration (pg/ml); *P=0.005 compared with controls at day 56 by Mann-Whitney U test. Sirtuin 1 (SIRT1) activity (**E**) and ACE2 (**F**) measured at the end of the study within SRA tissue of *ApoE*$^{-/-}$ mice receiving HFC versus HFC supplemented with resveratrol (RSV). Data expressed as median and interquartile range with maximum and minimum data points (whiskers) for deacetylase activity (relative fluorescence units; **E**) and tissue concentration (pg/µg protein; **F**).

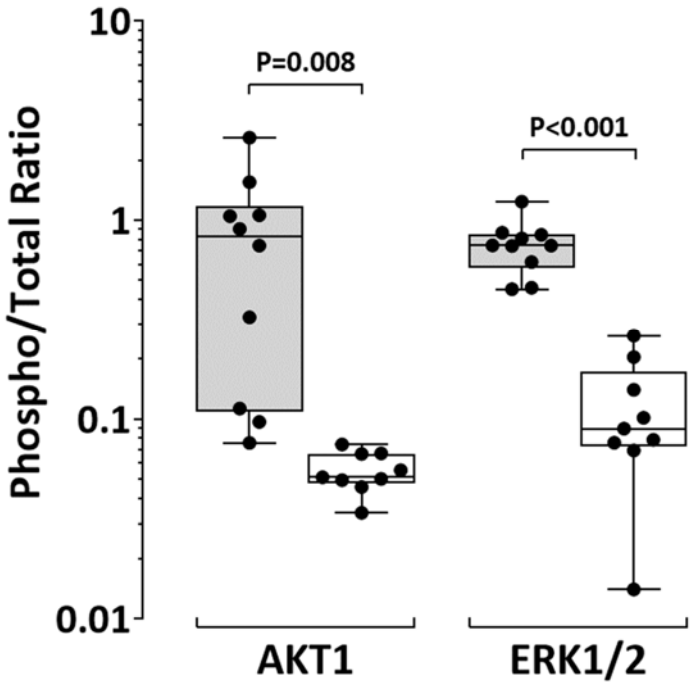

Figure 3: Resveratrol down-regulated aortic Akt and ERK1/2 phosphorylation in AngII-infused, high-fat fed *ApoE*$^{-/-}$ mice. Ratio of phosphorylated-to-total Akt1 and ERK1/2 in SRA tissue of mice fed control diet (grey) or resveratrol-supplemented diet (white). Data expressed as median and interquartile range with maximum and minimum data points (whiskers) for quantitative relation between phosphorylated and total kinase.

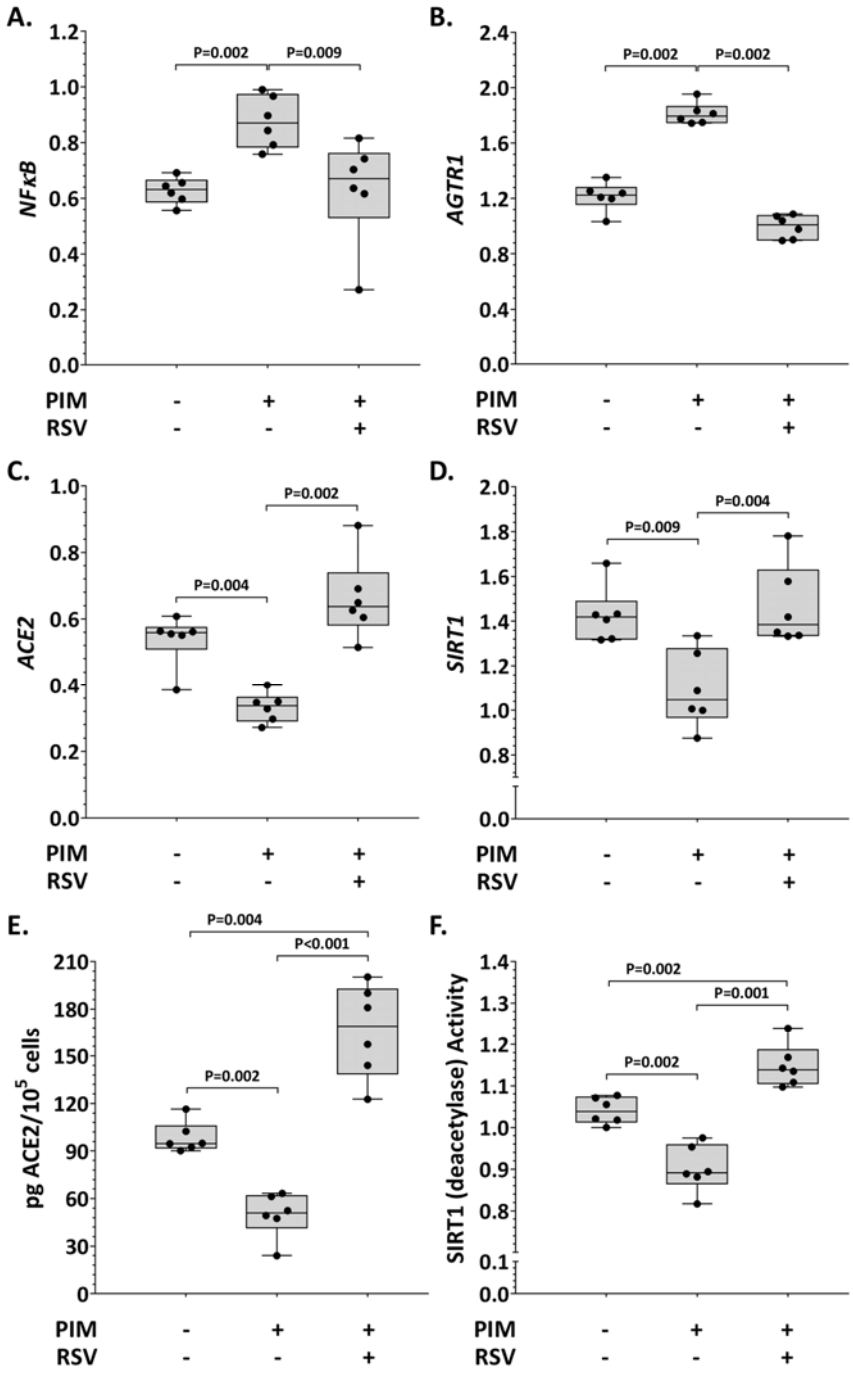

Figure 4: Effect of resveratrol (RSV) on inflammation-activated human AoSMC. Gene expression for *NFκB* (**A**), *AGTR1* (**B**), *ACE2* (**C**), and *SIRT1* (**D**), cellular ACE2 (**E**) and cellular SIRT1 activity (**F**) in a model of AoSMC inflammation induced by incubation of cultures in 10% v/v pro-inflammatory media (PIM) generated from lipopolysaccharide-stimulated monocytic THP-1 cells, and in the presence and absence of resveratrol (RSV; 5 μM). Data expressed as median and interquartile range with maximum and minimum data points (whiskers) for expression relative to *GAPDH* (**A**/**B**/**C**/**D**) or pg/10^5 cells (**E**), and deacetylase activity (relative fluorescence units; **F**).

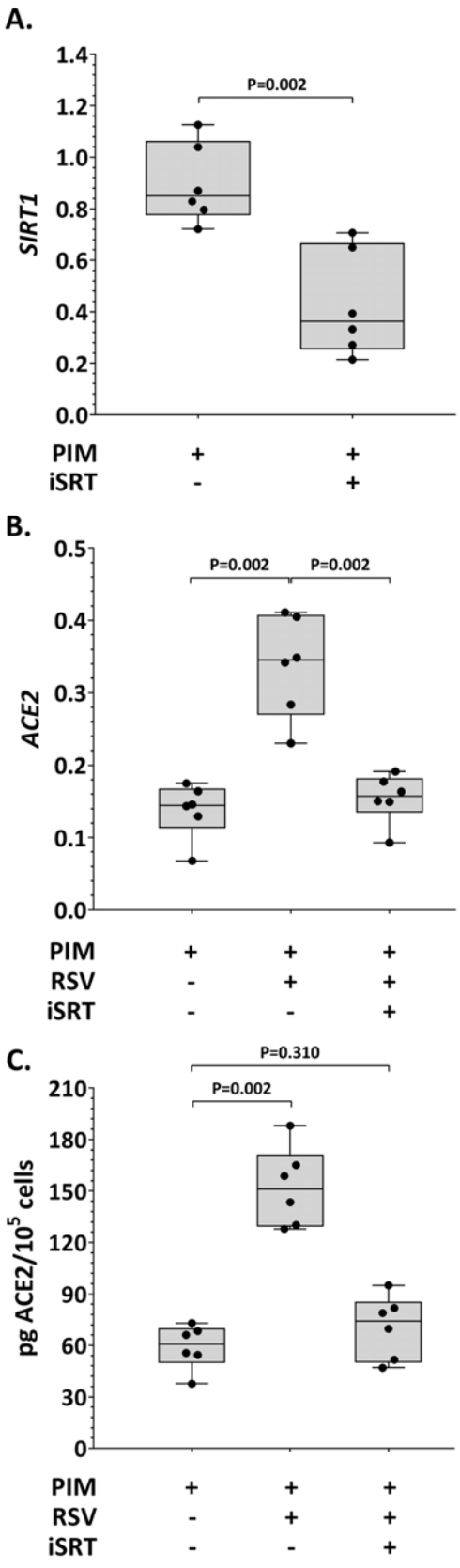

Figure 5: Sirt1-dependent up-regulation of ACE2 by resveratrol in inflammation-activated human AoSMC. A. siRNA-targeted silencing of *SIRT1* gene in a model of AoSMC inflammation induced by incubation of cultures in 10% v/v pro-inflammatory media (PIM). Data expressed as median and interquartile range with maximum and minimum data points (whiskers) for expression relative to *GAPDH*. Gene (**B**) and cellular (**C**) expression of ACE2 in inflamed AoSMC (PIM) in the presence and absence of resveratrol (RSV) and siRNA for SIRT1. Data expressed as median and interquartile range with maximum and minimum data points (whiskers) for expression relative to GAPDH (**B**) or pg/10^5 cells (**C**).

Table 1: Effect of resveratrol (RSV) on gene expression in pre-established, AngII-induced AAA in apolipoprotein E-deficient mice fed high-fat chow (HFC)

Gene	AngII+HFC (control)	AngII+HFC+RSV	Expression	P
	(n=11)	(n=14)		
Ace2	0.64 (0.49-0.92)	1.72 (1.12-2.49)	↑	0.008
Sirt1	1.81 (1.25-2.18)	2.86 (2.30-3.52)	↑	0.004
Nfkb1	3.26 (1.89-3.85)	0.72 (0.25-1.77)	↓	<0.001
Mmp9	1.99 (0.91-17.63)	0.74 (0.46-2.15)	↓	0.015
Mmp2	3.59 (2.21-7.98)	1.72 (0.40-2.76)	↓	0.067
Agtr1	2.67 (1.32-3.85)	1.17 (0.82-1.93)	↓	0.009

Data expressed as median (interquartile range) mRNA expression relative to Gapdh; P, two-sided p-value for comparison by Mann-Whitney U test. Ace2, angiotensin-converting enzyme 2; Agtr1, angiotensin II type-1 receptor; Nfkb1, nuclear factor of kappa light polypeptide gene enhancer in B cells 1; Mmp, matrix metallopeptidase; Sirt1, Sirtuin 1.

Table 2: Effect of resveratrol (RSV) over 24 hours on gene expression for *NFκB*, angiotensin II type 1 receptor (*AGTR1*), *ACE2*, and sirtuin 1 (*SIRT1*) in resting human AoSMC *in vitro*

Gene	Control	RSV	Expression	P
	(n=6 repeat cultures)	(n=6 repeat cultures)		
NFKB1	1.09 (0.99-1.20)	1.07 (0.94-1.19)	NC	0.937
AGTR1	1.82 (1.75-2.01)	0.94 (0.85-1.03)	↓	0.002
ACE2	0.59 (0.49-0.62)	0.64 (0.61-0.66)	↑	0.026
SIRT1	0.76 (0.73-0.91)	0.97 (0.94-1.07)	↑	0.064

Data expressed as median (interquartile range) mRNA expression relative to GAPDH; P, two-sided p-value for comparison between control and intervention by Mann-Whitney U test. NC, no change.

SUPPLEMENTAL MATERIAL

Resveratrol inhibits growth of experimental abdominal aortic aneurysm associated with upregulation of angiotensin converting enzyme 2

Moran CS, Biros E, Krishna SM, Wang Y, Tikellis C, Moxon JV, Cooper ME, Norman PE, Burrell LM, Thomas MC, Golledge J

Figures and Tables

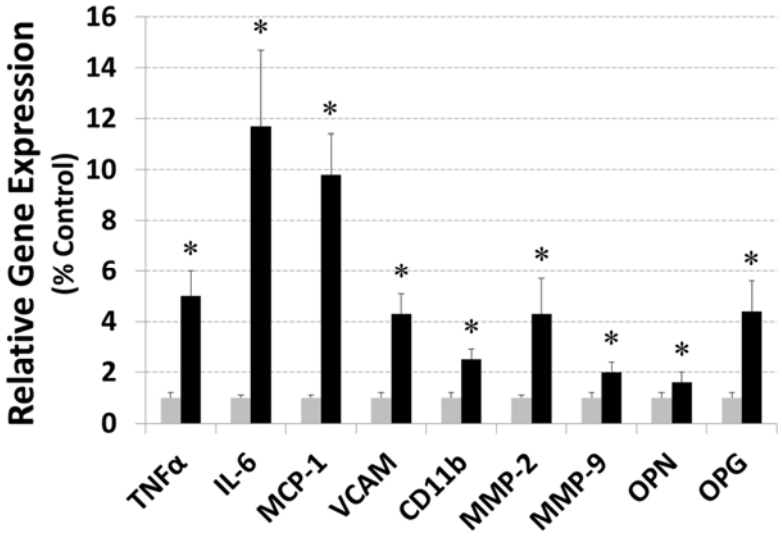

Figure I: Aortic expression of selected markers of vascular inflammation. Increased expression of genes associated with inflammation and proteolytic activity measured in the aortas of otherwise unmanipulated *ApoE*$^{-/-}$*Ace2*$^{-/y}$ mice. Data expressed as mean and SD expression relative to *ApoE*$^{-/-}$ controls (grey); * P<0.05, compared by unpaired t-test (n=8 per group). *IL,* interleukin; *MCP-1*, monocyte chemoattractant protein-1; *MMP*, matrix metalloproteinase; *OPG*, osteoprotegerin; *OPN*, osteopontin; *TNF*, tumor necrosis factor; *VCAM*, vascular cell adhesion molecule.

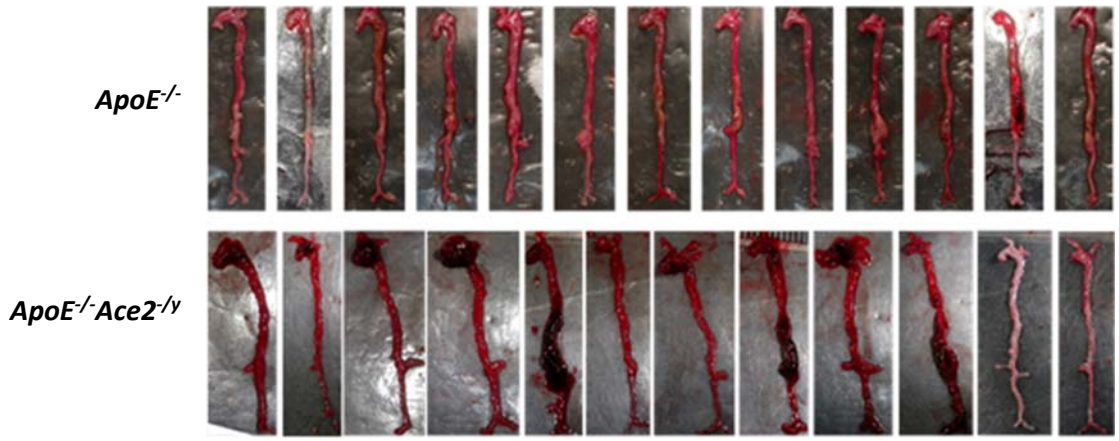

Figure II: Effect of Ace2 deficiency on aortic response to AngII. Gross morphology of aortas harvested from *ApoE*$^{-/-}$ (control) and *Ace2*-deficient (*ApoE*$^{-/-}$*Ace2*$^{-/y}$) mice infused with AngII over 28 days.

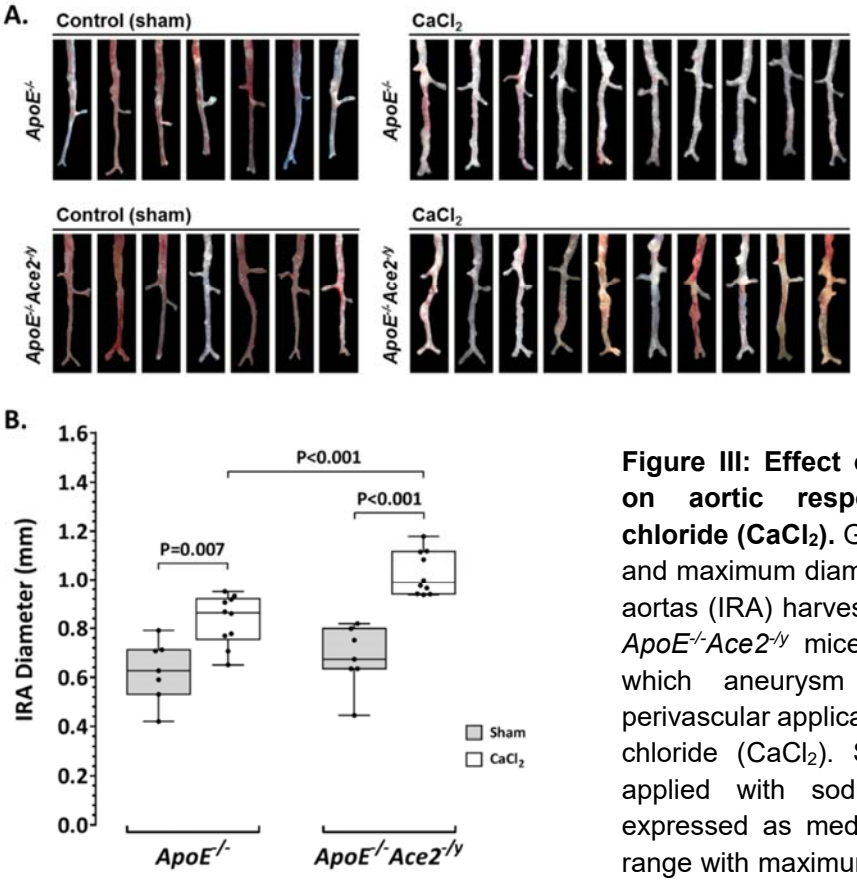

Figure III: Effect of ACE2 deficiency on aortic response to calcium chloride ($CaCl_2$). Gross morphology (**A**) and maximum diameter (**B**) of infrarenal aortas (IRA) harvested from *ApoE*$^{-/-}$ and *ApoE*$^{-/-}$*Ace2*$^{-/y}$ mice after 28 days, in which aneurysm was induced by perivascular application of 0.5 M calcium chloride ($CaCl_2$). Sham vessels were applied with sodium chloride. Data expressed as median and interquartile range with maximum and minimum data points (whiskers) for maximum diameter (mm).

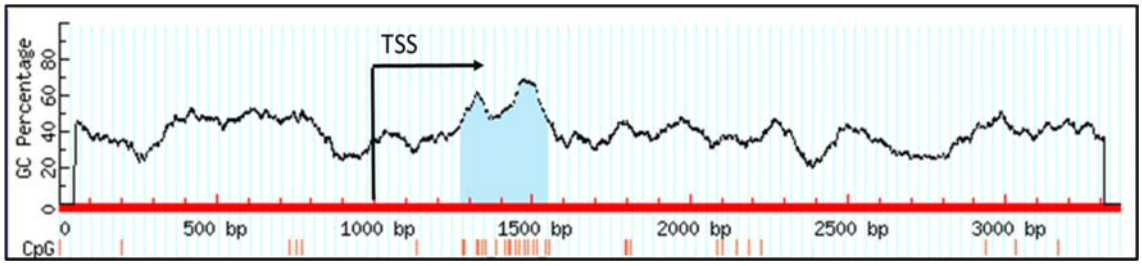

Figure IV: A schematic representation of the promoter region of ACE-2 gene. The red line denotes the input ACE-2 sequence along with 1000 base pairs (bp) upstream sequence from Transcription start site (TSS) submitted to the Methprimer software. The CpG islands are shown below the input sequence as red vertical lines.

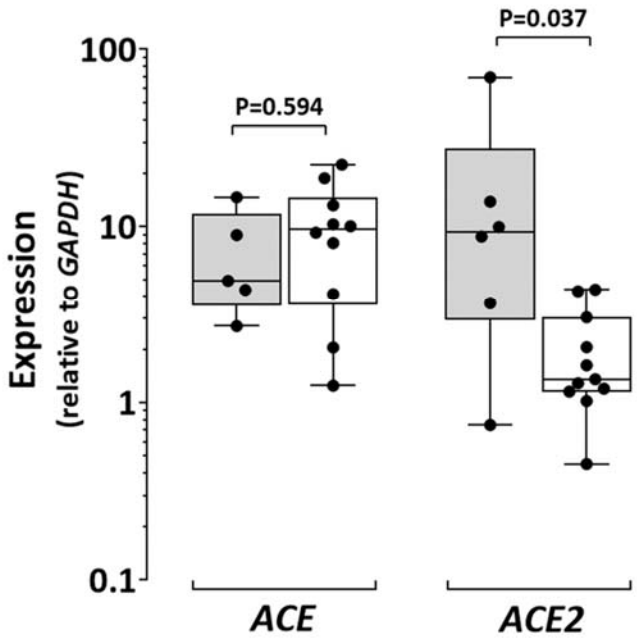

Figure V: Expression of *ACE* and *ACE2* in human AAA. Gene expression for ACE and ACE2 in infrarenal aortic biopsies collected from patients undergoing open surgery to repair abdominal aortic aneurysm (AAA; white bar) and from non-aneurysmal heart-beating brain dead organ donors (Control; grey bar). Data expressed as (log_{10}) median and interquartile range with maximum and minimum data points (whiskers) for expression relative to *GAPDH*.

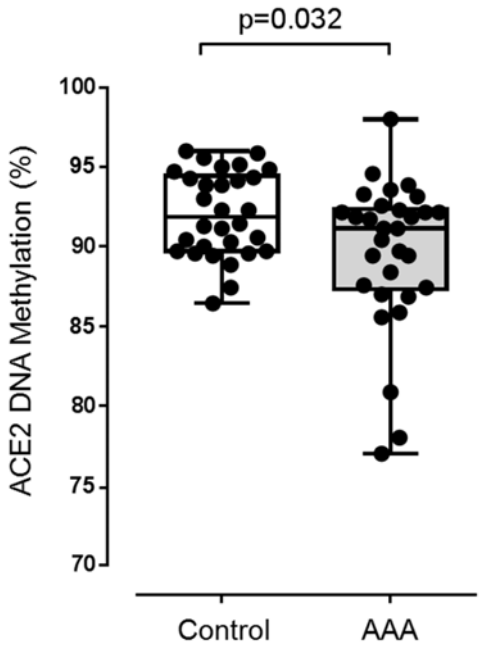

Figure VI: *ACE2* promotor DNA methylation. Methylation of CpG sites within the ACE2 promotor region in human infrarenal aortic biopsies collected from patients undergoing open surgery to repair abdominal aortic aneurysm (AAA; n=30) and from non-aneurysmal heart-beating brain dead organ donors (Control; n=30). Data expressed as median and interquartile range with maximum and minimum data points (whiskers) for percent methylation.

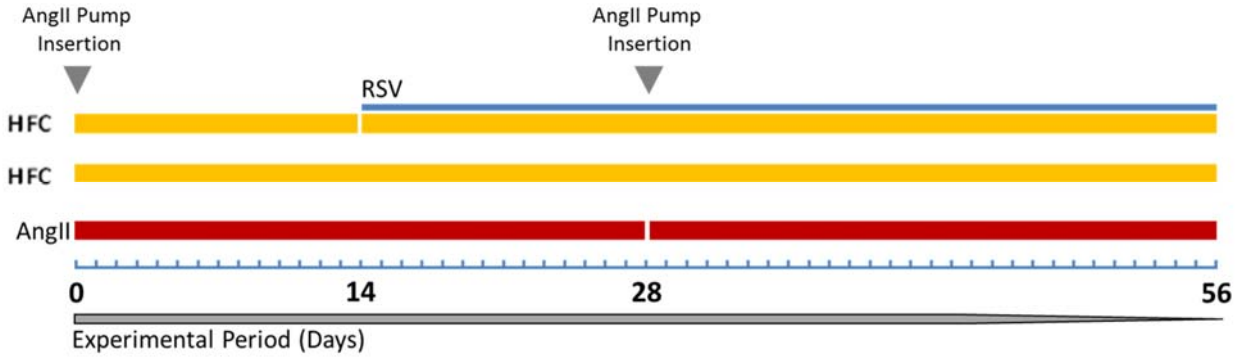

Figure VII: Study design and timeline over 56 days for resveratrol supplementation in AngII/*ApoE*$^{-/-}$ mouse model. Chronic infusion of AngII facilitated by using two 28-day subcutaneous ALZET minipumps. *HFC*, high-fat chow; *RSV*, resveratrol (HFC supplemented with 0.05 g resveratrol/100 g chow).

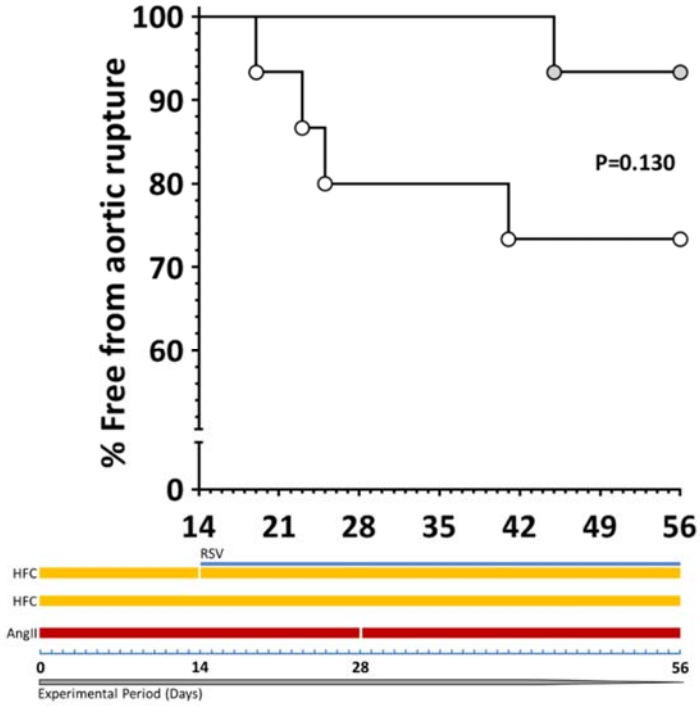

Figure VIII: Model survival. Kaplan-Meier curves of survival free from aneurysm rupture in a chronic model of AngII-induced AAA in which *ApoE*$^{-/-}$ mice were administered HFC diet (white; control) or HFC + 0.05 g resveratrol/100 g chow (grey) over 42 days. P-value calculated using Log-rank (Mantel-Cox) test.

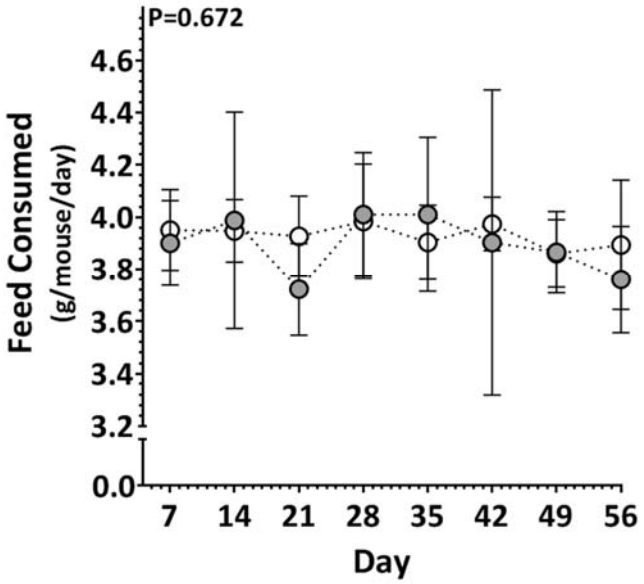

Figure IX: Consumption of diet. Average weekly consumption of feed by AngII-infused *ApoE*$^{-/-}$ mice administered HFC diet (grey; control) or HFC + 0.05 g resveratrol/100 g chow (white) over 42 days. Data expressed as mean and SD feed consumed (g/mouse/day) and compared using linear mixed effects.

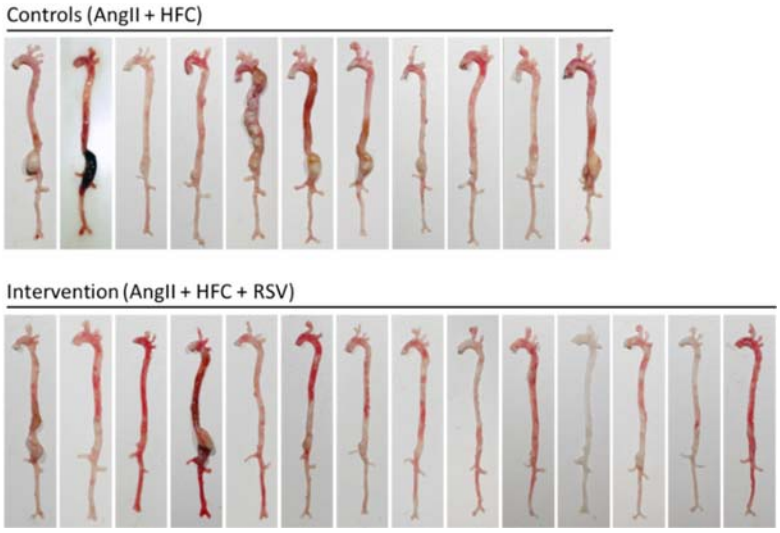

Figure X: Effect of resveratrol on aortic response in a chronic model of AAA. Gross morphology of aortas harvested from *ApoE*$^{-/-}$ mice in a chronic model of AngII-induced AAA administered either HFC diet (grey; control) or HFC + 0.05 g resveratrol/100 g chow (white) over 42 days.

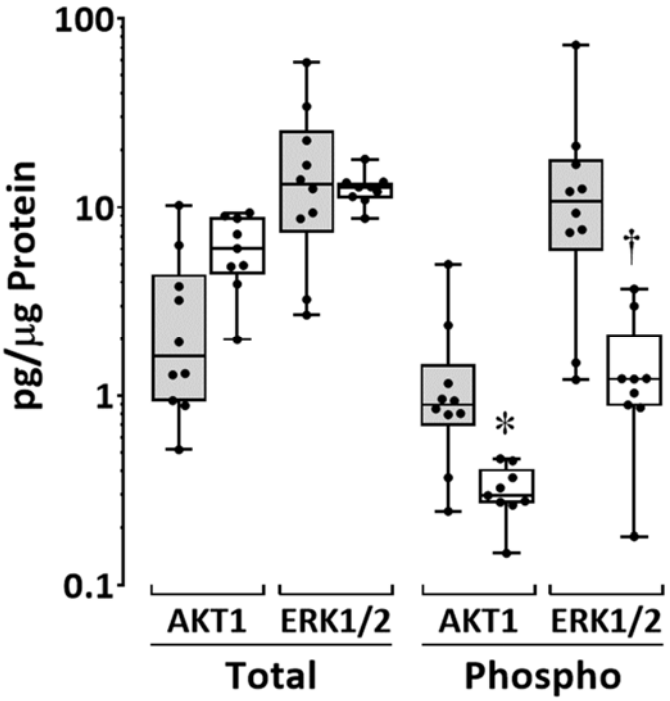

Figure XI: Akt1 and ERK1/2 phosphorylation in the SRA of AngII-infused, high fat-fed, *ApoE*$^{-/-}$ mice. Quantification of total and phosphorylated (Phospho) Akt1 and ERK1/3 in SRA tissue of mice receiving control diet (grey) or diet supplemented with resveratrol (white). Data expressed as median and interquartile range with maximum and minimum data points (whiskers) for tissue concentration (pg/μg protein); *P=0.003, †P=0.001.

Table I: Aortic expression of genes associated with matrix synthesis

Gene	*n*	*ApoE*$^{-/-}$	*ApoE*$^{-/-}$*Ace2*$^{-/y}$	P
Col1a1	8	1.0 ± 0.2	1.1 ± 0.2	>0.999
Col3a1	8	1.0 ± 0.1	1.3 ± 0.3	>0.999
Tgfb1	8	1.1 ± 0.3	1.0 ± 0.2	>0.999
Ctgf	8	1.0 ± 0.1	1.2 ± 0.1	>0.999
Fn1	8	1.0 ± 0.1	1.1 ± 0.1	>0.999
Eln	8	1.0 ± 0.2	0.9 ± 0.3	>0.999

Data expressed as Mean±SEM expression relative to Gapdh; P, two-sided p-value for comparison between control and intervention by Mann-Whitney U test. Col1a1, collagen 1; Col3a1, collagen III; Tgfb1, TGFβ; Ctgf, connective tissue growth factor; Fn1, fibronectin; Eln, elastin.

Table II: Characteristics of 548 HIMS participants in whom circulating ACE2 activity was measured

Characteristic	Whole Cohort (n=548)	Men without AAA (n=343)	Men with AAA (n=205)	P
Age (years)	72.0 (68.0-75.0)	72.0 (68.0-75.0)	71.0 (68.0-75.0)	0.537
Infra-renal aortic diameter (mm)	20.2 (19.2-32.2)	19.5 (19.2-20.2)	33.4 (31.6-38.1)	<0.001
BMI (kg/m^2)	26.6 (24.4-28.7)	26.4 (24.2-28.5)	27.0 (24.9-29.3)	0.009
Systolic blood pressure (mm/Hg)	155.0 (142.0-168.0)	156.0 (142.0-168.0)	153.0 (142.0-168.5)	0.513
Diastolic blood pressure (mm/Hg)	90.0 (81.0-97.0)	90.0 (81.0-97.0)	82.0 (90.0-99.0)	0.225
	History of			
Ever smoking	391 (71.4%)	217	174	<0.001
Diagnosed hypertension	218 (39.8%) [24]	122 (35.6%) [23]	96 (46.8%) [1]	0.043
Treatment for hypertension	182 (33.2%) [24]	94 (27.4%)	88 (42.9%)	0.001
Diagnosed diabetes	53 (9.7%) [1]	33 (9.6%)	20 (9.8%) [1]	0.944
Treatment for diabetes	52 (9.5%) [1]	32 (9.3%)	20 (9.8%) [1]	0.855
Diagnosed hyercholesterolaemia	214 (39.1%) [24]	126 (36.7%) [23]	88 (42.9%) [1]	0.393
Treatment for dyslipidaemia	126 (23.0%) [24]	68 (19.8%) [23]	58 (28.3%) [1]	0.061
Stroke	36 (6.6%) [24]	18 (5.2%) [23]	18 (8.8%) [1]	0.158
Myocardial infarction	93 (17.0%) [24]	43 (12.5%) [23]	50 (24.4%) [1]	0.001
Serum ACE2 activity (arbitrary fluorescence units)	712.1 (518.7-1044.7)	740.7 (529.2-1028.9)	688.5 (493.9-1047.2)	0.122

Continuous data shown as median and inter-quartile range, and are compared between groups using the Mann-Whitney U test. Categorical variables shown as count and percent, and are compared using the Chi-squared test. Square brackets denote the number of missing data points.

Table III: Association of serum ACE2 activity with AAA diagnosis by logistic regression

Covariate	Odds ratio	95% Confidence interval	P
Model 1: Unadjusted analysis			
ACE2 activity	0.849*	0.704-1.024	0.087
Model 2: Adjusted for risk factors for AAA, and differences observed between groups on univariate analysis			
ACE2 activity	0.808*	0.665-0.981	0.032
Age	1.139**	0.906-1.432	0.264
Ever smoking	3.181	2.009-5.037	<0.001
Diabetes	0.744	0.401-1.379	0.347
BMI	1.359***	1.123-1.645	0.002
History of hypertension	1.426	0.971-2.095	0.070
History of myocardial infarction	2.016	1.246-3.262	0.004

Odds ratio relates to a 1 std dev increase in serum ACE2 activity (529.5 (arbitrary fluorescence units)). ** Odds ratio relates to a 5-year increase in age; * Odds ratio relates to a 1 std deviation increase in BMI (3.3 units); For categorical variables, men who have the risk factor were compared to those who did not.*

Table IV: Characteristics of subjects for which *ACE2* promotor DNA methylation was assessed in infrarenal aortic biopsies

Characteristic	AAA	No AAA*	P
Number of individuals	30	30	-
Entry age (years)	70.8±3.6	42.7±13.6	<0.001
Aortic diameter (mm)	63.8±18.8	-	-
Body mass index (kg/m^2)	28.7±4.3	-	-
Male gender	12 (100%)	4 (67%)	0.098
Smoking history	8 (67%)	-	-
Hypertension	7 (58%)	-	-
Diabetes mellitus	1 (8%)	-	-
Coronary heart disease	4 (33%)	-	-
Dyslipidemia	7 (58%)	-	-

*Nominal variables presented as counts (percentage), and continuous variables presented as mean ± standard deviation (SD). Nominal and continuous variables compared between subjects using Fisher exact test and Mann Whitney U test, respectively. * Heart-beating brain dead organ donors.*

SUPPLEMENTAL MATERIAL

Resveratrol inhibits growth of experimental abdominal aortic aneurysm associated with upregulation of angiotensin converting enzyme 2

Moran CS, Biros E, Krishna SM, Wang Y, Tikellis C, Moxon JV, Cooper ME, Norman PE, Burrell LM, Thomas MC, Golledge J

Detailed Materials and Methods

Human AAA

This study was approved by the ethics committees of the Townsville Hospital and Health Services, James Cook University, the University of Western Australia and Leiden University Medical Center and the protocols conformed to the ethical guidelines of the Declaration of Helsinki.

Serum ACE2 activity: Five hundred and 48 participants of the Health In Men Study (HIMS) with available blood samples were included in the current study. The HIMS was a community-based screening trial for AAA and the protocols and cohort characteristics have been previously detailed [1]. Clinical information collected from each participant included age, smoking history, prior diagnosis, or treatment for hypertension, diabetes, dyslipidaemia, myocardial infarction or stroke, and blood pressure. Enzymatic activity of ACE2 in serum samples was measured by a fluorescence-based assay using the commercially available synthetic fluorogenic ACE2 substrate Mca-APK (Dnp) (Enzo, USA). A buffer solution containing 50mM MES, 300mM NaCl, 10µM ZnCl2, 1mM N-ethylmaleimide (NEM) (Sigma Aldrich) and 0.01% Triton X-100 (Labchem, Australia) was prepared and the pH of the buffer adjusted to 6.5. All the reactions were performed in duplicates in black 96 well plates with a total volume of 100µl. 50mM EDTA (Sigma Aldrich) was added to one of the duplicate wells and was constituted a blank. An inhibitor cocktail (Complete EDTA-free tablets; Roche, Switzerland) and 2mM phenylmethylsulfonyl fluoride (PMSF; Sigma Aldrich) were added to all the wells to prevent the hydrolysis of the ACE2 substrate by the non-metalloprotease enzymes potentially present in samples. Fluorescence was measured using the Enspire Multimode Plate Reader (Perkin Elmer, MA, USA) at 330-nm excitation and 400-nm emission wavelength following a 16-hour incubation on a shaker at room temperature. ACE2 activity was defined as the difference between the fluorescence measured in duplicate wells with and without EDTA addition.

Aortic ACE2 gene expression and ACE2 DNA methylation: Infrarenal aortic samples were collected from patients undergoing open surgery for AAA repair and from heart-beating brain dead organ donors (controls). Full thickness AAA biopsies (n=30) from the anterior wall of the aneurysm body (site of maximum aortic dilation) and juxtarenal aortic control samples (n=30) were snap frozen and stored in $^{-}80^{0}$C for DNA extraction. Aortic samples from a subgroup of 12 patients with AAA and six organ donors were stored in RNA later for total RNA extraction. Gene expression of *ACE2* (QT00034055; Qiagen) was assessed using quantitative real-time reverse transcription PCR. The relative expression of ACE2 in each sample was calculated by using the concentration-Ct-standard curve method and normalized using the average expression of glyceraldehyde-3-phosphate dehydrogenase (*GAPDH*; QT00079247; Qiagen). The ACE2 promoter region includes 12 CpG sites and methylation data obtained from the 12 sites were used for analysis. CpG islands in the promoter region of the ACE2 gene were identified using the MethPrimer software. Promoter specific methylation was assessed analysing PCR fragments by Sequenom MassArray and EpiTYPER software as previously reported [2]. The percentage of methylation for the ACE2 gene promoter was defined as the average of methylation values across the sample and presented as % CpG methylation [2].

Mouse models and *in vivo* studies

Approval for the animal studies was obtained from the local ethics committee and experimental work performed in accordance with the institutional and ethical guidelines of James Cook University, Australia (AEC approvals A2077 & A2358), and conformed to the Guide for the Care and Use of Laboratory Animals (National Institutes of Health, USA). Mice were housed in an individually-ventilated, temperature and humidity-controlled cage system (Aero IVC Green Line; Tecniplast) on a 12-hour light/dark cycle, and maintained on normal laboratory chow and water *ad libitum* until under experimental conditions.

Mice: Male *ACE2*-null apolipoprotein E-deficient (*ApoE*$^{-/-}$*Ace2*$^{-/y}$) mice and age and sex-matched *ApoE*$^{-/-}$ mice (both on a C57BL/6 genetic background) were generated as previously described [3].

AAA models: The angiotensin II (AngII) model was implemented as previously described [4,5]. Chronic infusion was facilitated using two osmotic micro-pumps (ALZET Model 1004, Durect Corporation) containing AngII (#A9525, Sigma-Aldrich) dissolved in sterile water, one inserted at day 0 and one at day 28, into the subcutaneous space left of the dorsal midline under anaesthesia (4% isoflurane), to administer AngII at a rate of 1.0 µg/kg/min continuously over 56 days. Induction of AAA by periaortic application of calcium chloride ($CaCl_2$) was performed as previously described [6]. Briefly, $CaCl_2$ solution (0.5 M) was applied for 15 minutes to the adventitia of the infra-renal abdominal aorta (IRA) exposed under 4% isoflurane anaesthesia. Sham controls underwent a similar procedure except 0.9% sodium chloride was applied to the IRA adventitia in place of $CaCl_2$.

Intervention diet: High-fat chow (HFC; modified AIN93G semi-pure rodent diet SF08-043 (45% calculated energy from ghee, 1.25% cholesterol) supplemented with trans-resveratrol (Chem-Supply, Australia; 0.05 g per 100 g HFC) was prepared by a commercial supplier (Specialty Feeds, Australia).

Studies: Four separate studies were performed:

i) Baseline cardiovascular parameters in ApoE$^{-/-}$*Ace2*$^{-/y}$ *mice.* Protein and molecular analyses of serum and suprarenal aorta (SRA), and blood pressure, were compared between otherwise unmanipulated 14-week old male *ApoE*$^{-/-}$ (n=6) and *ApoE*$^{-/-}$*Ace2*$^{-/y}$ mice (n=6).

ii) Effect of ACE2 deficiency on AngII-induced AAA. 14-week old male *ApoE*$^{-/-}$*Ace2*$^{-/y}$ mice (n=12) and *ApoE*$^{-/-}$ controls (n=13) were infused with AngII (1.0 µg/kg/min) over 28 days.

iii) Effect of ACE2 deficiency on $CaCl_2$-induced AAA. AAAs were induced in 14-week old male *ApoE*$^{-/-}$*Ace2*$^{-/y}$ mice (n=10) and *ApoE*$^{-/-}$ (n=10) controls by perivascular application of 0.5 M $CaCl_2$ and mice assessed over 28 days.

iv Effect of resveratrol on ACE2 and growth of pre-established AAAs. 14-week old male *ApoE*$^{-/-}$ mice were chronically infused with AngII (1.0 µg/kg/min) over an eight-week period. After an initial 14-day AAA establishment period, mice were allocated to HFC (control; n=15) and HFC + 0.05 g resveratrol/100 g chow (intervention; n=15) groups for the remaining six weeks. Allocation was based upon ultrasound measurement of SRA diameter such that median and interquartile range were similarly matched between the two groups.

Assessment of experimental AAA

Maximum diameter of the SRA (from the aortic hiatus to the left renal artery) and IRA (from left renal artery to the aortic bifurcation) was determined by morphometric analysis *ex vivo*, while *in vivo* diameter of these arterial segments was monitored by ultrasound as previously described [6]. Necropsy was performed within 24 hours of sudden mouse fatality to confirm aortic rupture as the cause of death. Phosphate buffered saline-perfused aortas were harvested from mice completing the study protocol and were placed on a graduated template and digitally photographed (Coolpix 4500, Nikon). Maximum SRA and IRA diameters were determined from the images using computer-aided analysis (Adobe®

Photoshop® CS6 Extended version 13, Adobe Systems Incorporated). Ultrasound measurements of the IRA (*study iii*) were obtained prior to $CaCl_2$ application (day 0) then weekly throughout the study (day 7, 14, 21, and 28). Ultrasound measurements of the SRA (*study iv*) were obtained prior to AngII infusion (day 0) and every two week throughout the study (day 14, 28, 42 and 56). Scans were performed in sedated mice (4% isoflurane) using a MyLabTM 70 VETXV platform (Esaote, Italy) with a 40 mm linear transducer at an operating frequency of 10 MHz (LA435; Esaote, Italy) to provide a sagittal image of the SRA. Maximum outer wall SRA diameter was measured at peak systole using the calliper measurement feature. Good inter-observer reproducibility of morphometric and ultrasound analysis has been demonstrated previously in our laboratory [6].

Blood Pressure

Blood pressure was measured using a computerized, non-invasive, tail-cuff system (Kent Scientific, USA). Animals were habituated to the device before measuring the pressures to ensure accurate measurements. Good reproducibility of this technique has been established previously (mean of absolute difference for mean blood pressure: 12.3 mmHg, 95% CI: 8.4–16.1) [7].

Measurement of angiotensin II

Serum and aortic concentrations of AngII were measured in *ApoE*$^{-/-}$ and *ApoE*$^{-/-}$*Ace2*$^{-/y}$ mice using a commercially available radioimmunoassay (ProSearch International, Malvern) as per the manufacturer's instructions as previously described [8].

Serum cholesterol and triglycerides

Circulating concentrations of cholesterol and triglyceride were determined in serum samples from *ApoE*$^{-/-}$ and *ApoE*$^{-/-}$*Ace2*$^{-/y}$ mice using the automated Abbott Architect ci8200an platform (Abbott Laboratories, USA).

Aortic lysyl oxidase activity

Aortic activity of lysyl oxidase (LOX) was measured in *ApoE*$^{-/-}$ and *ApoE*$^{-/-}$*Ace2*$^{-/y}$ mice using the commercially available Amplite™ Fluorimetric Lysyl Oxidase Assay (AAT Bioquest® Inc.) as per the manufacturer's instructions.

Cell culture

Healthy human aortic vascular smooth muscle cells (AoSMC; Clonetics® human aortic SMC, Lonza) were seeded at $1x10^5$ cells/ml into separate cultures and maintained in Dulbecco's Modified Eagle Medium (DMEM; Sigma-Aldrich) supplemented with 10% fetal bovine serum (FBS; Gibco). Cells were growth arrested at ~90% confluency by incubation in DMEM + 0.1% FBS overnight (18 hours). Chronic inflammation-induced activation of cells was modelled by incubation of cultures in DMEM + 10% FBS comprising 10% v/v conditioned media generated from human monocytic THP-1 cells exposed to 10 μg/ml endotoxin (Lipopolysaccharide; Sigma-Aldrich) over a period of five days (control cells, n=6 repeat cultures). Experimental cultures (n=6 repeat cultures) were exposed to the same pro-inflammatory media but supplemented with resveratrol (5 μM; R5010, Sigma-Aldrich) over the final 24-hour period. Gene silencing of *Sirt1* was performed using small interfering (si) RNA (FlexiTube siRNA, SI00098434, Qiagen) added to culture 48 hours prior to cell harvest. Harvested cells were prepared for protein and molecular analysis.

Measurement of ACE2

A commercially available sandwich high sensitivity ELISA was used to determine the concentration of ACE2 protein expressed in cultured human AoSMC (EK0997, Boster

Biological Technology) and in serum and the suprarenal aorta (SRA) of experimental mice (EK1188, Boster Biological Technology), as per the manufacturer's instructions. Gene expression for ACE2 in mouse SRA was determined by quantitative real-time PCR.

Measurement of Sirt1 activity

Cellular and aortic Sirt1 deacetylase activity was measured in cultured human AoSMC and experimental mice, respectively, using a commercially available activity assay (CS1040, Sigma Aldrich) as per the manufacturer's instructions. The two-step protocol involved first the deacetylation by Sirt1 of an acetylated lysine side chain-containing substrate, followed by cleavage of the deacetylated substrate by a developing solution and release of a highly fluorescent group. The measured fluorescence was directly proportional to the deacetylation activity of the enzyme within the sample.

Measurement of Aortic AKT1 and ERK1/2

Protein from SRA samples harvested at the end of the study was extracted by homogenisation in RIPA buffer (Sigma-Alrdrich) and the concentration determined using Bradford reagent (Bio-Rad Laboratories) according to the manufacturer's recommendations. Measurement of phosphorylated and total AKT1 (AKT 1/2/3 (pS473) + Total AKT1) and ERK1/2 (ERK1/2 (pT202/Y204) + Total ERK1/2; Abcam) was performed using a SimpleStep ELISA™ (Abcam) as per manufacturer's instructions.

Quantitative real-time PCR

QuantiTect® Primer Assays were used to determine gene expression for *ACE2* (QT00034055), *Sirt1* (QT00051261), *NFKB1* (QT00063791), and *AGTR1* (QT00233548) in human tissue samples and AoSMC, and *ACE2* (QT00111293), *Sirt1* (QT01055642), *Nfkb* (QT00154091), *Agtr1* (QT00261464), *Col1a1* (QT00162204), *Col3a1* (QT01055516), *Tgfb1* (QT00145250), *Ctgf* (QT00096131), *Fn1* (QT00135758), *Eln* (QT01070482), *Il6 (*QT00098875), *Tnf* (QT00104006), *Ccl2* (QT00167832), *Vcam1* (QT00128793), *Itgam* (QT00116116), *Spp1* (QT00157724), *Tnfrsf11b* (QT00116116), *Mmp2* (QT00116116) and *Mmp9* (QT00108815) in mouse aortas using quantitative real time (qPCR) as previously described [9]. The relative expression of these genes in experimental and control samples was calculated by using the concentration-Ct-standard curve method and normalized using the average expression of glyceraldehyde-3-phosphate dehydrogenase (human *GAPDH*, QT00079247; mouse *Gapdh*; QT01658692) for each sample using the Rotor-Gene Q operating software version 2.0.24. The QuantiTect SYBR® Green one-step RT-PCR Kit (Qiagen) was used according to the manufacturer's instructions with 40ng of total RNA as template. All reactions were independently repeated in duplicate and the mean of the two values for each sample was used for analyses.

Statistical analysis

Data were analysed using GraphPad Prism (version 6) and TIBCO Spotfire S+ (version 8.2). D'Agostino and Pearson's test was used to test normality of the data, and parametric or non-parametric tests were applied appropriate to data distribution. Comparison of *in vitro* end-point data was performed using Mann-Whitney *U* test. For animal studies, aortic end-point data for maximum diameter and protein or gene expression were compared between control and intervention animals by Mann-Whitney *U* test. Comparison between baseline and end-point serum or tissue concentrations was performed within each mouse group using paired-t test, while % change relative to baseline for control and intervention was compared by

Mann-Whitney *U* test. Mouse data obtained as a function of time (ultrasound of SRA diameter, body-weight) was compared within each group by repeat measures one-way ANOVA, and between control and intervention mice by mixed-effects linear regression (MLE). Kaplan-Meier survival curves were analysed using log-rank (Mantel-Cox) test. In all cases P values less than 0.05 were considered significant.

References

1. Norman PE, Flicker L, Almeida OP, Hankey GJ, Hyde Z, Jamrozik K. Cohort Profile: The Health In Men Study (HIMS). Int J Epidemiol 2009;38:48-52.
2. Krishna SM, Seto SW, Jose RJ, Li J, Morton SK, Biros E, Wang Y, Nsengiyumva V, Lindeman JH, Loots GG, Rush CM, Craig JM, Golledge J. Wnt Signaling Pathway Inhibitor Sclerostin Inhibits Angiotensin II-Induced Aortic Aneurysm and Atherosclerosis. Arterioscler Thromb Vasc Biol 2017;37:553-566.
3. Thomas MC1, Pickering RJ, Tsorotes D, Koitka A, Sheehy K, Bernardi S, Toffoli B, Nguyen-Huu TP, Head GA, Fu Y, Chin-Dusting J, Cooper ME, Tikellis C. Genetic Ace2 deficiency accentuates vascular inflammation and atherosclerosis in the ApoE knockout mouse. Circ Res 2010;107:888-897.
4. Moran CS, Jose RJ, Biros E, Golledge J. Osteoprotegerin deficiency limits angiotensin II-induced aortic dilatation and rupture in the apolipoprotein E-knockout mouse. Arterioscler Thromb Vasc Biol 2014;34:2609-2616.
5. Moran CS, Rush CM, Dougan T, Jose RJ, Biros E, Norman PE, Gera L, Golledge J. Modulation of Kinin B2 Receptor Signaling Controls Aortic Dilatation and Rupture in the Angiotensin II-Infused Apolipoprotein E-Deficient Mouse. Arterioscler Thromb Vasc Biol 2016;36:898-907.
6. Krishna SM, Seto SW, Moxon JV, Rush C, Walker PJ, Norman PE, Golledge J. Fenofibrate increases high-density lipoprotein and sphingosine 1 phosphate concentrations limiting abdominal aortic aneurysm progression in a mouse model. Am J Pathol 2012;181:706-718.
7. Seto SW, Krishna SM, Moran CS, Liu D, Golledge J. Aliskiren limits abdominal aortic aneurysm, ventricular hypertrophy and atherosclerosis in an apolipoprotein-E-deficient mouse model. Clin Sci (Lond) 2014;127:123-134.
8. Tikellis C, Bialkowski K, Pete J, Sheehy K, Su Q, Johnston C, Cooper ME, Thomas MC. ACE2 deficiency modifies renoprotection afforded by ACE inhibition in experimental diabetes. Diabetes 2008;57:1018-1025.
9. Biros E, Walker PJ, Nataatmadja M, West M, Golledge J. Downregulation of transforming growth factor, beta receptor 2 and Notch signaling pathway in human abdominal aortic aneurysm. Atherosclerosis 2012;221:383-386.